The Vesta Mk 2 rate of fire spread model

a user's guide

CSIRO

Fire Behaviour Characteristics Chart

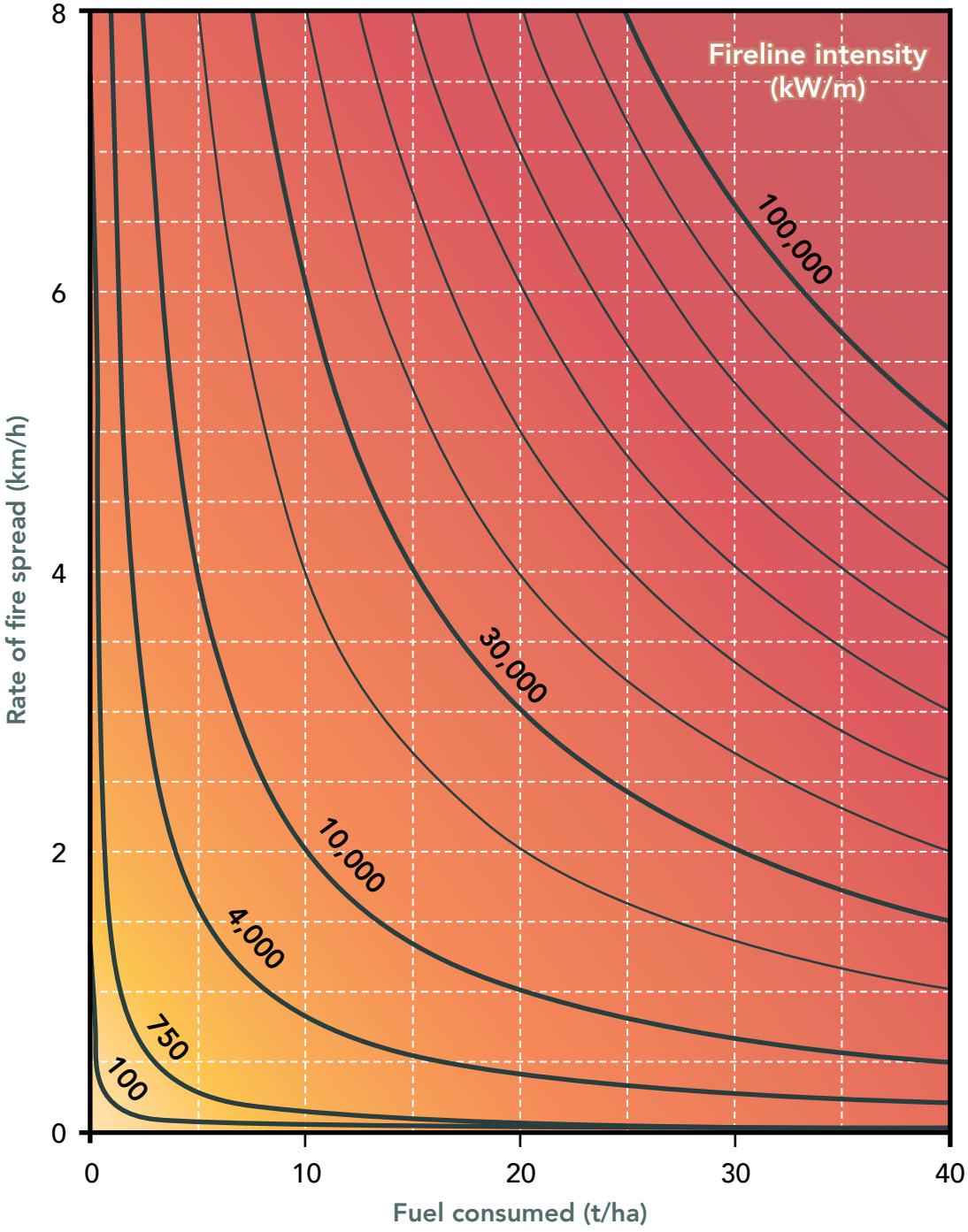

Rate of fire spread unit equivalencies

km/h	0.06	0.12	0.18	0.24	0.3	0.6	0.9	1.2	1.8	2.4	3.0	3.6	4.2	4.8	5.4	6.0	7.5	9.0
m/min	1	2	3	4	5	10	15	20	30	40	50	60	70	80	90	100	125	150

The Vesta Mk 2 rate of fire spread model

a user's guide

Miguel G. Cruz

2021

Enquiries should be addressed to:
Miguel Cruz
CSIRO
GPO Box 1700, Canberra ACT 2601
Email: miguel.cruz@csiro.au

Citation

Cruz, MG (2021) The Vesta Mk 2 rate of fire spread model: a user's guide. CSIRO, Canberra, ACT. 76 pp.

Cover illustration by Jen Hollis.

Acknowledgments

This research was funded by the State Government of New South Wales and the CSIRO. We thank Simon Heemstra, Laurence McCoy and Stuart Matthews for their support of the work that led to the development of the Vesta Mk 2 fire spread model. The current publication benefited from extensive feedback provided by numerous fire behaviour analysts on the usage of the model namely David Field and David Philp. Thanks also to Marty Alexander, Stuart Matthews, Musa Kilinc, Tom Duff, Matt Plucinski and Andrew Sullivan for their comments on earlier drafts of this guide.

Thanks to Kathryn Steel for the design and production of this guide.

Table of contents

Foreword

Fire behaviour modelling is an important function within the NSW RFS and was vital during the 2019-20 fire season where fire behaviour analysts used a range of models to prepare more than 4,500 predictions of fire behaviour.

The development of the Dry Eucalypt Forest Fire Model (Project Vesta) in 2012 enabled us to provide predictions of forest fire behaviour in elevated Fire Danger when compared to other traditional fire behaviour models.

One impediment to widespread use of this model was the requirement for more detailed fuel information. This can be difficult to obtain without detailed knowledge or information of the fuels being consumed by the fire. Research undertaken for Vesta Mark 2 has helped to simplify and reduce the model's sensitivity. These improvements will greatly assist Fire Behaviour Analysts right through to firefighters on the ground.

One of the other challenges for applying the Vesta model is its range of applicability. This was evident during the 2019-20 fire season where the extremities of weather and fire behaviour meant that no single fire behaviour model was applicable for predictions in forest vegetation formations. Fire Behaviour Analysts had to use their knowl*edge*, skills and experience of existing models to determine which model was applicable during the fluctuations of fire escalation and de-escalation. Improvements to the model range of applicability will reduce the need for interchange between models.

Finally, for NSW RFS Fire Behaviour Analysts, discerning fire escalation and the need for incremental use of fuel strata to date has been governed largely by experience and expert judgement. Whilst this still has a role to play in predicting fire behaviour, having access to a more repeatable and rigorous method will assist to improve fire behaviour predictions. More rigorous science undertaken by this project will provide analysts with more guidance for incorporating fuel into predictions of fire behaviour.

We believe that the improvements to Vesta Mark 2 model will provide many benefits to the management of fire in NSW, with the ultimate outcome being improved safety for our firefighters and the wider community.

We thank you for undertaking this important research and we are looking forward to working with CSIRO to implement the new model.

Yours Sincerely,

Deputy Commissioner Kyle Stewart
Preparedness and Capability
NSW Rural Fire Service

1 Introduction

Reliable models for calculating the speed at which a wildfire front can advance across the landscape are essential to enable accurate predictions of fire behaviour. Such information is needed in order to devise suitable suppression strategies for fire containment and to enable the preparation and timely releases of effective public warnings.

Over the years a number of models have been developed that aim to quantify the expected rate of spread of fires in eucalypt forests. A few of these have found operational application for the prediction of wildfire propagation, namely the "Guide for Control Burning in Eucalypt Forest" (also known as 'Leaflet 80', McArthur (1962)), the McArthur Forest Fire Danger Meter (McArthur 1967); the Western Australian Forest Fire Behaviour Tables (the WA 'red book', Sneeuwjagt and Peet (1985)) and the Dry Eucalypt Forest Fire Model (Project Vesta, Cheney *et al.* (2012)). Details of these models are given in 'A Guide to Rate of Fire Spread Models for Australian Vegetation' (Cruz *et al.* 2015). These models, occasionally with some adaptations, have also been implemented in various landscape fire spread simulation software used in Australia, such as Phoenix Rapidfire, Aurora and Spark.

The Vesta Mk 2 rate of fire spread model for eucalypt forests builds upon the strengths and advantages of previous models and addresses several identified operational constraints. This model was developed to enable the operational prediction of the forward rate of spread of fires burning in eucalypt forests and across a broad range of fire spread potential and intensities. A description of the development of the model, its features, and a detailed evaluation, are given in Cruz *et al.* (2022).

The purpose of this guide is to provide a systematic methodology for predicting the spread rate and behaviour of fires in eucalypt forests using the Vesta Mk 2 model. The guide includes an overview of the model, considerations on the input variables and a description of their potential effects on the model outputs. Simplified tabular outputs of the model are provided to allow a first approximation to fire spread potential in the absence of computer software.

Box 1. Project Vesta

Project Vesta was a research project conducted by CSIRO and WA Department of Conservation and Land Management between 1996 and 2001 with the financial and practical support of all state land management agencies and rural fire authorities. The aim of this project was to develop a national forest fire behaviour prediction system suitable for use in all dry eucalypt forests under dry summer conditions (Gould *et al.* 2007a). The final version of this model was published in 2012 and became known colloquially as the Vesta model. The fire spread model for eucalypt forests presented here, Vesta Mk 2, draws from the previous model analysis and the fire behaviour dataset originally collected during Project Vesta.

2 Fire behaviour in eucalypt forests

Eucalypt forests in Australia encompass a broad range of vegetation communities and fuel types. Common traits in these fuel types are the presence of a dominant overstorey tree layer, seldom exceeding 30 m in height in dry open forests but which can be taller in wet eucalypt forests; a canopy cover greater than 30%; and a diverse understorey comprised of shorter trees, shrubs, sedges and grasses. As a fuel complex, the eucalypt forest presents multiple fuel layers or strata. From the bottom up, these have been typically described as (Figure 1): surface (duff, litter, twigs and detached bark laying on the forest floor); near-surface (grasses, low shrubs, creepers, and suspended dead leaf, twig and bark from overstorey vegetation; note – certain Australian jurisdictions consider the near-surface fuels as part of the surface fuel layer); elevated (taller shrubs); bark fuel attached to tree stems; intermediate tree canopy; and overstorey tree canopy.

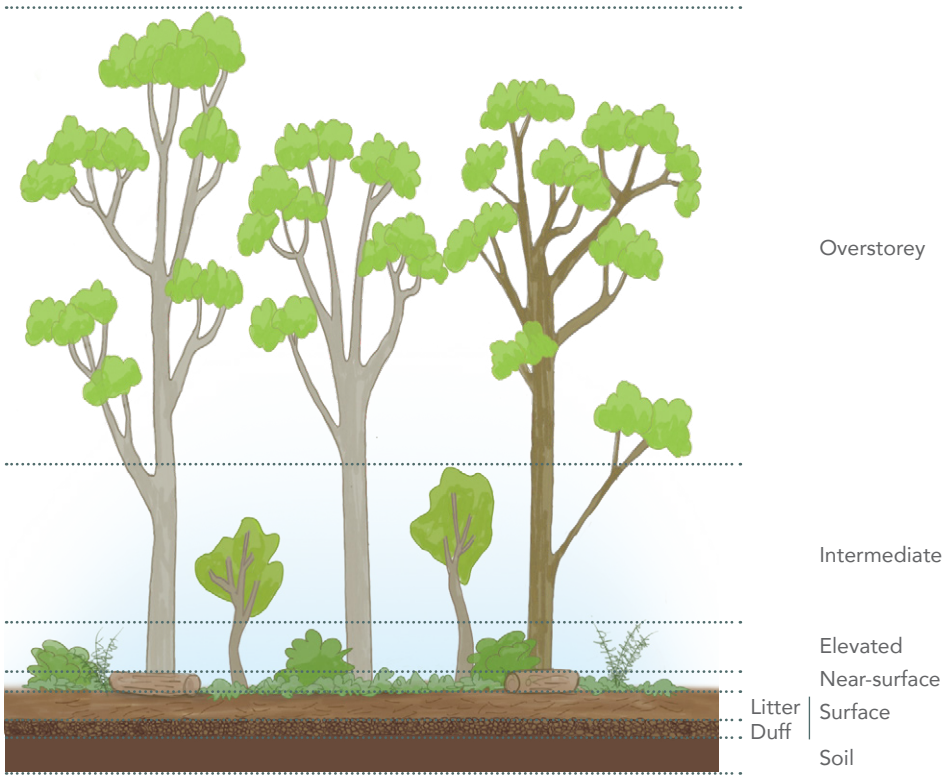

Figure 1. Illustration of the various fuel layers that can define a eucalypt forest fuel complex. Based on illustration from Gould *et al.* (2007a)

A fire spreading under dry summer conditions within a multi-layered fuel complex, such as a dry sclerophyll eucalypt forest with a shrubby understorey will, depending on burning conditions, involve different fuel layers in the combustion and propagation processes. Changes in fuel or environmental conditions (*e.g.*, an increase in wind speed or decrease in fuel moisture) will allow the flame front to transition vertically from the surface and near-surface layers into the elevated shrub component, and then into the intermediate and overstorey fuel strata. The presence of fibrous bark on some species provides connectivity (*i.e.*, a 'ladder' fuel) between the understorey and overstorey fuel layers. Fibrous bark particles are easily ignited allowing for vertical fire propagation and potential for profuse spot fire ignitions after detachment from the main tree stem.

As a fire transitions into these higher fuel strata, there will be a stepwise increase in its forward rate of spread and intensity (Figure 2). This is typically associated with an increased efficiency of heat transfer into taller, vertically-oriented fuel layers; enhanced radiant heating owing to taller and deeper flames; increased exposure to wind flow; and an increase in the amount of firebrands detached and transported ahead of the flame front. The most dramatic changes are observed when a flame front spreading in understorey fuels transitions into a state where overstorey fuels become involved, *i.e.*, a so-called 'crown fire'. Under conditions that enable the transition of an understorey fire to a crown fire, spotting becomes the dominant process of fire propagation in eucalypt forests (McArthur 1967; Luke and McArthur 1978), and a fire may double its spread rate compared to its previous state. Over its full range of fire behaviour, wildfires in dry eucalypt forests will vary from mild surface fires with flames no taller than a few centimetres to fully developed crown fires with fireline intensities exceeding 50,000 kW/m and flames extending well above the overstorey canopy.

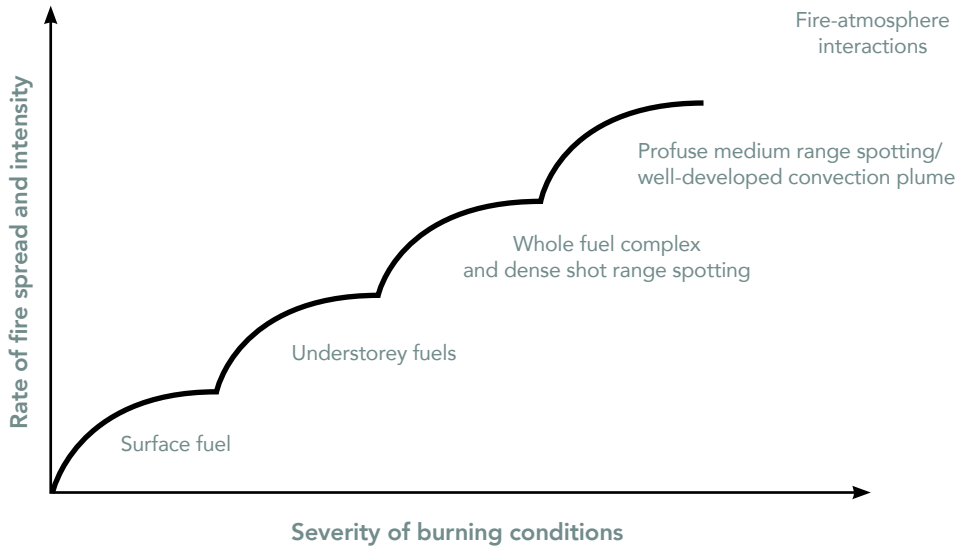

Figure 2. Conceptual stepwise increase in rate of fire spread and intensity as distinct fuel layers become involved in combustion processes. Based on illustration from McArthur (1967).

3 The Vesta Mk 2 rate of fire spread model

The Vesta Mk 2 rate of fire spread model considers, for practical purposes, that there are three distinct phases of fire propagation in eucalypt forests (Table 1):

(i) a low intensity state (Phase I);

(ii) a moderate to high intensity state (Phase II); and

(iii) a very high and greater intensity state (Phase III).

Phase I fire propagation is a low intensity state where a fire spreads via combustion of litter, or surface, and near-surface fuels under nil to low wind speeds or moderate to high dead fuel moisture contents (Figure 3).Taller shrub vegetation (*i.e.,* elevated fuels) not in contact with the surface litter and bark fuels attached to the tree stems are not typically involved in the flaming combustion process contributing to the propagation of the flame front, although they may burn collaterally behind the flame front. Average flame heights are typically less than 1.0 m high and propagation, generally less than 0.12 km/h (< 2 m/min), is controlled by the heat transfer processes occurring within the surface and near-surface fuel layers (Table 1).

Figure 3. Example of Phase I fire propagation (low intensity) in an open eucalypt forest with a well-developed surface and near-surface layer and a dense shrub understorey.

Phase II fire propagation encompasses moderate to high intensity fires driven by the combustion of understorey shrubs and a proportion of bark attached to tree stems (Figure 4). Rates of spread will typically range from 0.12 km/h (2 m/min) up to 1.5 km/h (25 m/min). The combustion of elevated and bark fuel layers allows more efficient transfer of energy from the flame front into unburned fuels ahead of the fire, leading to an increase of the effect of wind speed on the rate of fire spread. Short to medium range spot fire activity is expected to occur, but only becoming significant as a fire propagation mode in the upper range of this phase.

Table 1. Fire spread dynamics in eucalypt forests

Fire propagation phase		
Phase I	**Phase II**	**Phase III**
Defining characteristics		
Low intensity surface fire Small flames	Moderate to high intensity understorey fire Understorey shrub fuels involved Ignition of bark on tree trunks Combustion of canopy fuels possible in upper range of phase	Very high intensity fire involving whole fuel complex Short range spotting Canopy combustion likely
Fuels involved		
Litter Near-surface	Litter Near-surface Elevated Bark	Litter Near-surface Elevated Bark Canopy
Fire spread mechanisms (by order of importance)		
Radiation within fuel bed Flame contact	Convection Flame contact Radiation Short to medium range spot fire at upper end of range	Convection Flame contact Radiation Concentrated, high density medium range spotting / spot fire coalescence at upper end of range.
Indicative range in rate of fire spread (km/h)		
<0.12	0.12 – 1.5	>1.5
Indicative fireline intensity class (kW/m)		
10 - 300	300 - 7500	>7500

Phase III propagation represents the highest intensity state of fire behaviour associated with wildfires involving the full fuel complex, from the surface to the overstorey (Table 1). Fires in this state are characterised by very high fireline intensities and tall flames often reaching above the top of the canopy (Figure 5). The propagation of the flame front is driven by the coupling of profuse short-range spotting and coalescence of individual spot fires and flame front heat transfer processes, such as radiation and convection (incorporating hot gas advection and flame contact). Within this phase the dominance of short- and medium-range spotting increases as wind speed increases. In the upper range of intensity in this phase, typically associated with strong wind speeds and critically dry fuels, the high density of short- and medium range spotting can cause the formation of pseudo-flame fronts from coalescing spot fires and fire-storm like effects, where there is typically no single fire front as such, but multiple simultaneous burning zones that appear to be chaotically spreading in different directions. The higher energy release rates associated with this phase lead to a feedback mechanism that causes a proportion of fuels other than fine to be consumed in the flame front, increasing the overall intensity of the fire.

Figure 4. Examples of fire propagation within the lower (top) and upper (bottom) range of Phase II. (photos: top, Jennifer Hollis; bottom, CSIRO).

Figure 5. High intensity fire spreading in Phase III in an open eucalypt forest involving the full fuel complex in combustion (photo: Wayne Rigg, CFA).

In order to adequately cover the full range in rate of fire spread, the Vesta Mk 2 model considers the propagation in each phase separately, with each phase being described by a specific rate of fire spread equation. The system also quantifies the transition between phases by calculating the likelihood or probability of a phase occurring given a set of burning conditions.

The Vesta Mk 2 model has seven inputs (Table 2), directly incorporating the effect of wind speed, fine dead fuel moisture content, the load of surface and near-surface fuels, understorey fuel structure, and slope steepness (relative to the spread direction). Long-term landscape dryness as estimated by the McArthur (1967) Drought Factor is used to estimate fuel availability. A wind adjustment factor associated with a specific forest types is also required.

Table 2. Vesta Mk 2 rate of fire spread model inputs

Variable	Typical source
10-m open wind speed (km/h)	Weather forecast or onsite observations
Wind adjustment factor (dimensionless)	Estimated from forest fuel type
Fine dead fuel moisture content (%)	Estimated from a separate sub-model using air temperature and relative humidity (measured or forecasted), time of day and season; can be measured directly
Drought Factor (0-10, dimensionless)	Calculated from a model using measured or forecasted rainfall to 9 am, number of days since last rain and estimate of soil dryness using either the Keetch-Byram Drought Index (KBDI) or the Mount Soil Dryness Index (SDI)
Fuel load (t/ha)	Quantity of fine fuels in the surface and near-surface layers; estimated from fuel type and time since fire or directly measured
Understorey fuel height (m)	Calculated from near-surface and elevated fuel height and cover
Slope steepness (degrees or percent)	Estimated from maps or digital terrain models

The flowchart presented in Figure 6 illustrates how the various components of the model are linked, including direct inputs (solid boxes), the associated calculations of intermediate input quantities (orange boxes) such as fuel availability and fine dead fuel moisture content, the calculation of phase likelihoods (*i.e.* the probability a fire is spreading in a given fire propagation phase) and associated rate of fire spread. The rate of fire spread calculated for a given set of input conditions is the average of the various rates of spread ($R(i)$, where i is the spread phase) weighted by the likelihood of each phase occurring ($P(i)$). Details on the computational method and equations used are given in Section 9 – Equations and calculation procedures.

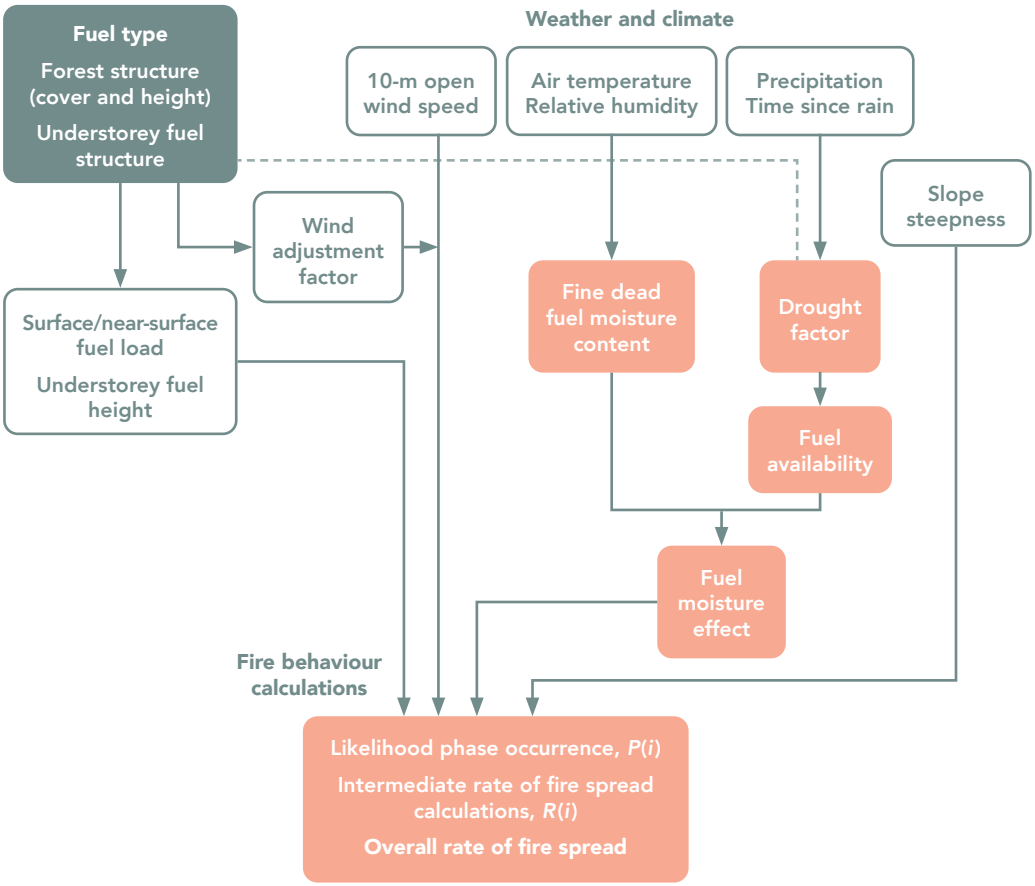

Figure 6. Diagram of the flow of data in the Vesta Mk 2 model for predicting the forward spread rate of fire in eucalypt forests. $P(i)$ is the probability of a certain fire propagation phase (i, II or III) to occur and $R(i)$ is the rate of spread for phase i (I, II or III).

Given the distinct fuel layers driving fire propagation in each phase, the effect of fuel characteristics on rate of spread, the energy outputs and heat transfer efficiencies will differ for each phase. As such, each rate of spread phase model responds differently to the effect of wind speed, fine dead fuel moisture content and fuel structural characteristics. Figure 7 illustrates how the three rate of fire spread *R*(*i*) models respond to increases in wind speed alone, and how the system links the various models *R*(*i*) to produce a final predicted rate of fire spread.

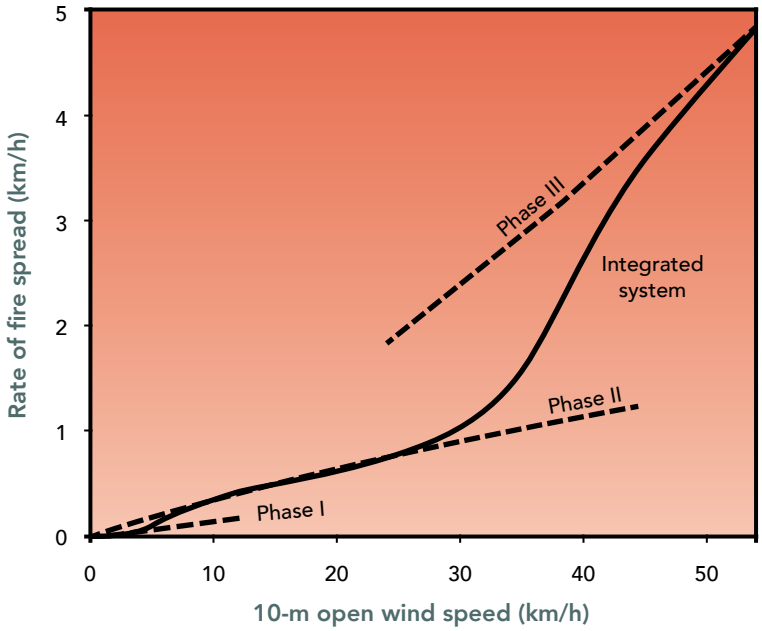

Figure 7. Modelled rate of fire spread in eucalypt forests as a function of wind speed as described by the three propagation phase rate of spread functions and the system used to integrate or unify them into a continuous relationship.

4 Input description

4.1 Wind speed

Wind is not only one of the most significant factors driving fire propagation, but it is also the most variable, with its magnitude and direction changing spatially (Figure 8) and temporally over a range of scales, from metres and seconds to kilometres and hours. The wind that affects the spread and behaviour of fire in eucalypt forests results from a complex interaction between the atmosphere, the terrain and the structure of the forest, particularly the height and density of its canopy. Understanding of how general or prevailing winds driven by a particular synoptic situation interact with more localised orographic, frontal or differential influences, such as those driving slope and valley winds, sea breezes, and the possible occurrence of spurious winds, is necessary to better integrate forecasted wind data with the reality of a site-specific fire spread prediction.

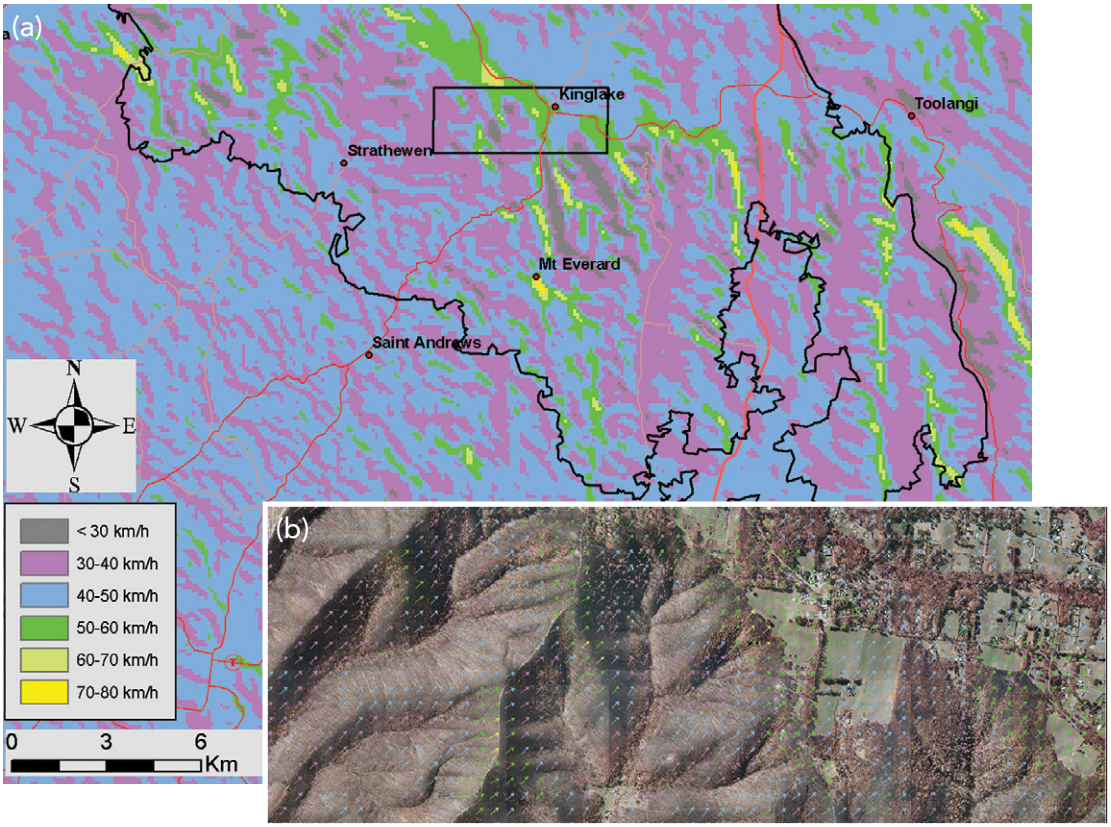

Figure 8. Visualisation of simulated spatial variation in wind strength (a) and direction (b) for an area of the 2009 Kilmore East fire, Victoria.

The Vesta Mk 2 model requires knowledge of the wind speed in the form of:

- the mean wind speed measured at the standard 10-m in the open and averaged over a period of at least 10 minutes;
- mean within-forest stand wind speed, assumed to be at eye-level height or at a nominal height of 1.7 to 2.0-m.

A fire propagation prediction will require forecasted wind information. The best source for the mean 10-m open wind speed is the forecasted wind as provided by the Bureau of Meteorology or other commercial weather forecasting services. Conversion between the 10-m open and the understorey wind speeds requires assumptions about the vertical wind profile under the canopy which is a function of several factors, namely forest structure and canopy architecture, understorey development, position in the slope and wind exposure, atmosphere stability and the speed of the wind itself. For an expedited model application, Table 3 below summarises typical wind adjustment factors (*WAF*) that enable a direct conversion between the 10-m open and the understorey wind speed, with the latter obtained by dividing the open wind speed by the *WAF*. The values in Table 3 are only indicative. Higher values can be found for tall/wet forests.

Table 3. Wind adjustment factors (*WAF*) to estimate 2-m within stand wind speed in eucalypt forests of different heights and canopy covers from a forecasted or measured 10-m open wind speed. Divide the forecast or measured 10-m open wind speed by the *WAF* to convert to an under-canopy wind speed

Stand canopy cover (%)	Stand height (m)		
	5 – 10	10 – 30	>30
<30	2.5	2.8	3.0
30 – 60	2.8	3.0 * 3.4 in fuel types with tall shrubs present	4.0 * 4.5 in fuel types with tall shrubs present
>60	4.0	4.5	5.0 * 6.5 in multi-strata stands with dense mid-storey

Directly measured wind data is also of great utility, namely to adjust and validate forecasted winds, or as a source of wind information in the absence of forecasted weather or if the forecast is not representative of the fire location. If measured wind speed and direction information is used, care should be taken that measurements comply with standard assumptions (*e.g.*, the wind is measured in the open at, or, corrected to a height of 10-m and averaged over at least 10 minutes). Direct measurements of understorey winds can also be extrapolated to the idealised open situation using the WAF value in Table 3. Care should be taken to ensure localised effects are considered when extrapolating wind speed measured at a particular location to a broader region, specifically ensuring adequate positioning of the instrument in regard to potential sheltering and aspect/slope position, so wind measurements are not biased. The measurements should be averaged over a period of at least 10 minutes and ideally longer to ensure it covers more than one wind gust/lull cycle and is thus relevant to the period over which any fire spread prediction is intended to be applicable. In the absence of any forecasted wind or measured data, the modified Beaufort wind scale (inside back cover) can be used as an approximation of wind strength based on direct *in situ* observations.

The effect of 10-m open wind speed on the Vesta Mk 2 fire spread output is illustrated in Figure 9. The effect of wind speed is dependent on the phase dominating fire propagation, with the effect being lowest for fires spreading in Phase I and highest for fires spreading in Phase III. The higher effect found for the latter likely arises from the effect of firebrand transport and spot fire ignition in driving headfire propagation in high intensity wildfires in eucalypt forests. The model sensitivity to wind speed is increased as a fire transitions between phases. The overall effect will also depend on other fire environment variables, as illustrated by the distinct curve trajectories for different fine dead fuel moisture contents in Figure 9.

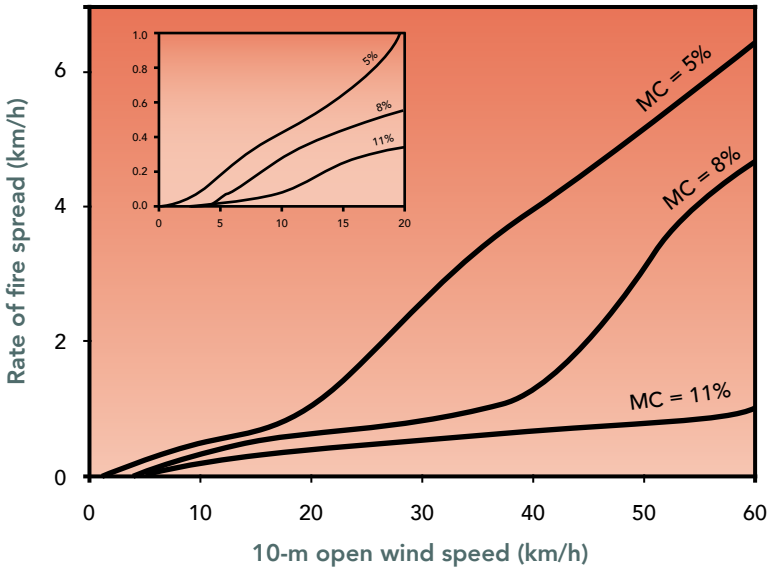

Figure 9. The effect of 10-m open wind speed on the fire spread rate in Vesta Mk 2 model for three different fine dead fuel moisture content values. Simulations are based on the following fixed inputs: W_s = 11 t/ha, h_u = 0.5 m, slope steepness = 0°, *WAF* = 3.3, and *DF* = 10.

Box 2. Relative sensitivity

Relative sensitivity was calculated to understand how the model responds to perturbations, or uncertainty, in input conditions. The relative sensitivity used considers a 10% variation in the input and quantifies the percent change in the model rate of fire spread output. A relative sensitivity of 10% indicates that the model output changed by 10% for the set 10% change in the selected input variable. Such an equivalent response indicates the model to be sensitive to that variable. Lower values will indicate the model to be less sensitive or, at a lower extreme, insensitive to the input variable. Higher relative sensitivity suggests the model to be more sensitive to variation in the input variable. Open to interpretation is what constitutes under or over sensitivity to one input over a range of burning conditions. For example, a 30% change in the output from a 10% increase in wind speed might be reasonable for a certain range of burning conditions where the fire spread rate is sensitive to small changes in wind speed.

Figure 10 shows the distribution of the sensitivity of model output (% change in rate of fire spread) to a 10% change in wind speed for a broad range in predicted rate of fire spread. The figure shows that the sensitivity to wind speed varies as the rate of fire spread increases, being lower for the low spread rates and increasing for faster spreading fires. On average, the sensitivity is close to the 10% change threshold, but in certain situations the sensitivity increases to values close to 20%. Higher sensitivity variation is observed for the <0.5 km/h and 2.0 to 4.0 km/h rate of fire spread classes due to the transition between phases, namely from I and II for the lower spreading class and II and III for the latter.

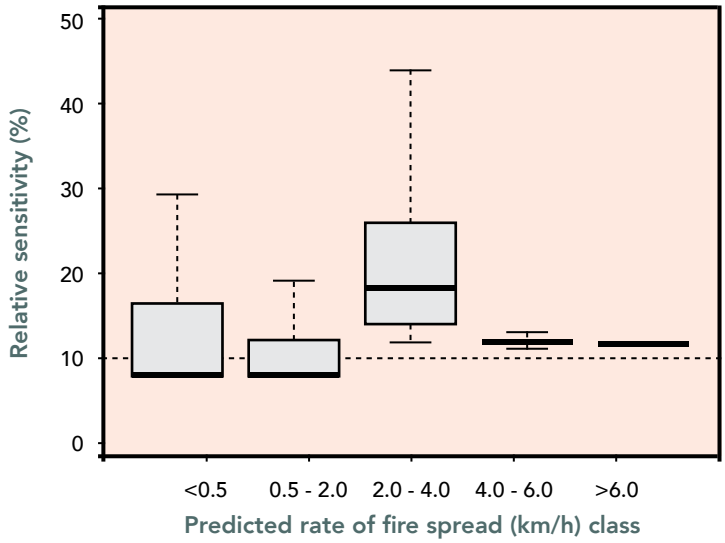

Figure 10. Distribution of relative sensitivity of the Vesta Mk 2 model to a 10% change in the 10-m open wind speed input as a function of the predicted rate of fire spread grouped into 5 classes. The solid line in each box indicates the median. Each box defines the interquartile range. The solid horizontal lines outside each box show the maximum and minimum values (excluding outliers). The dashed horizontal line indicates a sensitivity equal to that of the change in the input value.

4.2 Moisture content of fine dead fuels

Fuel moisture describes the amount of water present in the fuel. It is normally expressed as a percentage of the fuel's oven-dry weight. The moisture in fuels acts as a heat sink in the combustion process, with moister fuels requiring more energy to burn. In eucalypt forests the moisture content of fine dead fuels can have a significant impact on fire propagation, affecting the pre-heating and ignition of unburned fuels, spot fire occurrence, combustion processes, smoke production and the overall energy released. When the dead fuel moisture content is around 20%, the amount of moisture in the fuel will constrain fire spread, and may cause flaming combustion to self-extinguish. When fuel moisture is below about 6%, the dryness in fine dead surface fuels will allow for easy ignition and in turn the potential for widespread spot fire occurrence. The Vesta Mk 2 model describes this effect through the dead fine dead fuel moisture factor (Figure 11). This factor is bounded between 0.0 (self-extinguishment at 24% moisture content) and 1.0 (maximum effect reached when the fine dead fuel moisture is below 4.1%). As moisture of the upper litter layers reaches the assumed moisture of extinction of 24%, active flaming combustion is likely to self-extinguish. Nonetheless, glowing, and residual combustion of lower organic fuel layers, or other fuels such as coarse woody debris, may continue if their moisture contents allow. The movement of the combustion interface in these fuels will nonetheless result in a negligible rate of fire spread. The combustion of these fuels could enable the fire to rekindle when the moisture content of the upper litter layer drops again below the moisture of extinction threshold.

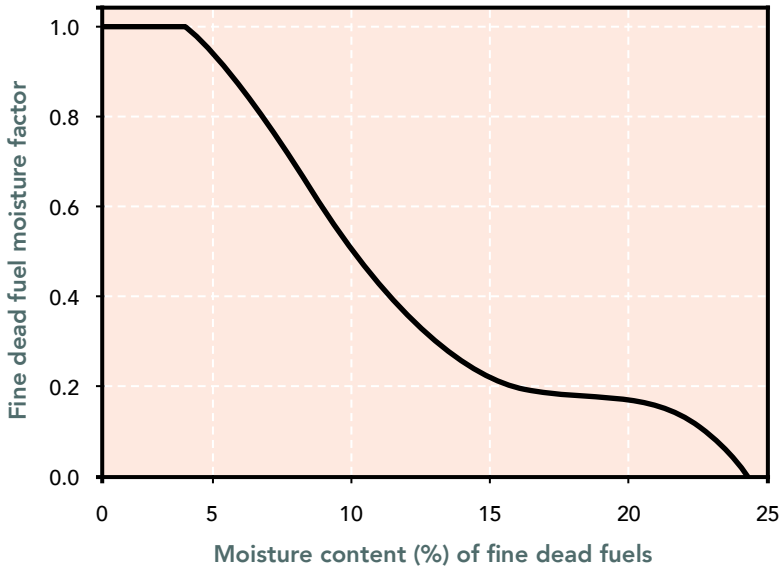

Figure 11. The effect of fine dead fuel moisture content on the spread rate of fire in the Vesta Mk 2 model works through the fine dead fuel moisture factor.

Dead fuels exchange moisture with the surrounding environment, as dictated by the moisture in the atmosphere, air temperature, solar radiation and the presence of free water on the surface of the fuel. In the dry conditions typically associated with summer-time wildfire propagation, the moisture content of fine dead fuels will follow the diurnal pattern of changes in air temperature and relative humidity (Figure 12), with higher values occurring overnight and lower values typically found throughout the mid-afternoon period (characterised by higher air temperature and lower relative humidity).

Fuel moisture content can be directly sampled, inferred from analogues (*e.g.*, electronic moisture meters) or predicted by a model. The use of the Vesta Mk 2 model as a predictive tool will require estimation of fine dead fuel moisture content using models that take into consideration forecasted atmospheric conditions, time of the day and the moisture content of deep fuel layers. The Matthews (2006) process-based fuel moisture model has been found to produce unbiased estimations of the moisture content of eucalypt litter and near-surface fuels. Simplified equations have been derived that approximate fuel moisture content from air temperature, relative humidity, time of the day and season. Tables M1 and M2 (Section 10 – Fire behaviour tables) provide tabular outputs from these equations for a range of discrete environmental conditions.

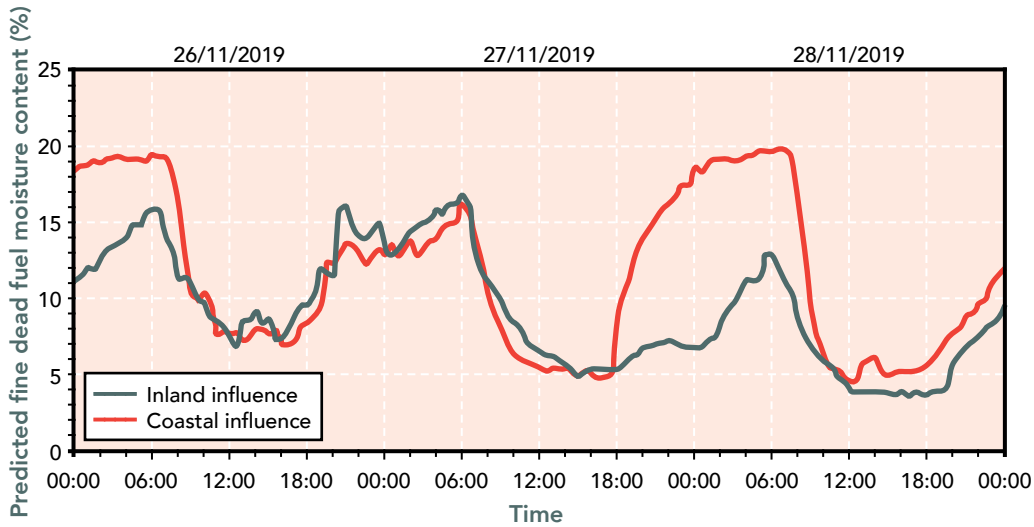

Figure 12. Modelled diurnal variation in fine dead fuel moisture content over a three day period for two sites 30 km apart subjected to a more humid coastal (red) and drier inland (black) weather influence.

It should be noted that this approximation for predicting dead fuel moisture content of the litter of an open eucalypt forest works best for periods when the forest floor fuel layers are homogeneously dry, as would be found in the mid to late stages of a fire season. A steep moisture gradient in the litter and duff layer profiles, with the lower layers having significantly higher moisture contents than the surface layers (as would be expected to occur sometime after a rainfall event or during spring and autumn or in tall, wet forest), will likely result in the moisture contents of upper litter and near-surface dead fuels to be higher than indicated by Tables M1 and M2. In these situations, actual fine dead fuel moisture content could be 1 to 2 % higher than that given by the tables. Canopy cover and aspect can also result in discrepancies between the values predicted by the tables and reality. The effect of high overnight relative humidity or dew formation on the moisture content of dead fuels is also not captured in Tables M1 and M2. In these situations, detailed modelling using the full moisture content model of Matthews (2006) will likely be required to obtain more accurate estimates of the moisture content of fine dead fuels.

The effect of moisture content on the Vesta Mk 2 fire spread outputs through the fine dead fuel moisture factor is illustrated in Figure 13. The overall effect will depend on other fire environment variables, such as fuel load and structure, landscape dryness, and the phase in which the fire is spreading.

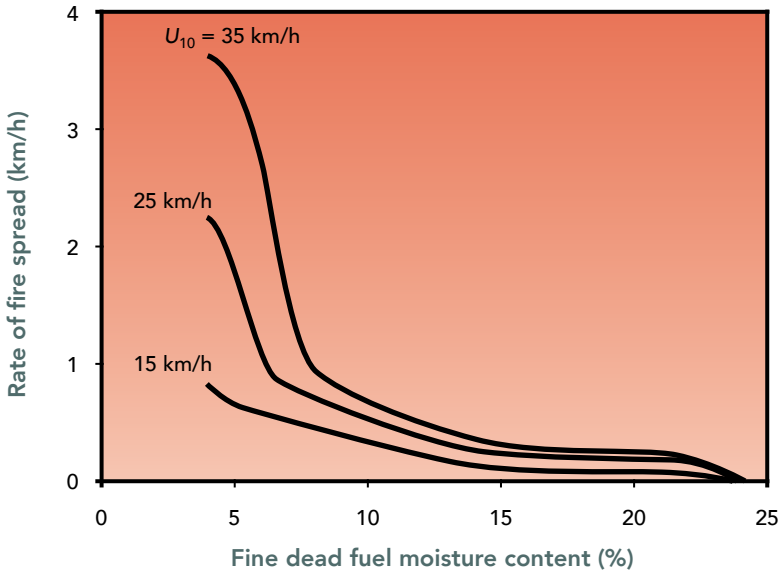

Figure 13. The effect of fine dead fuel moisture content on the fire spread rate in Vesta Mk 2 model for three different 10-m open wind speeds. Simulations are based on the following fixed inputs: W_s = 11 t/ha, h_u = 0.5 m, slope steepness = 0°, *WAF* = 3.3, and *DF* = 10.

Figure 14 shows the sensitivity (%) of the model to a 10% change of in fine dead fuel moisture content for five rate of fire spread classes. The results show the increase in fuel moisture content causes a reduction in predicted rate of fire spread (*i.e.*, negative sensitivity). The model is most sensitive, with a percent change in rate of spread larger than the percent change in dead fuel moisture content, to changes in fuel moisture when fires are spreading at less than 4 km/h. Above this value, the relative sensitivity in percent is less than the change in the input value. As with the dynamics observed in the effect of 10-m open wind speed, the 2.0 to 4.0 km/h rate of fire spread class shows a wider distribution, a result of the transition between Phase II and Phase III propagation.

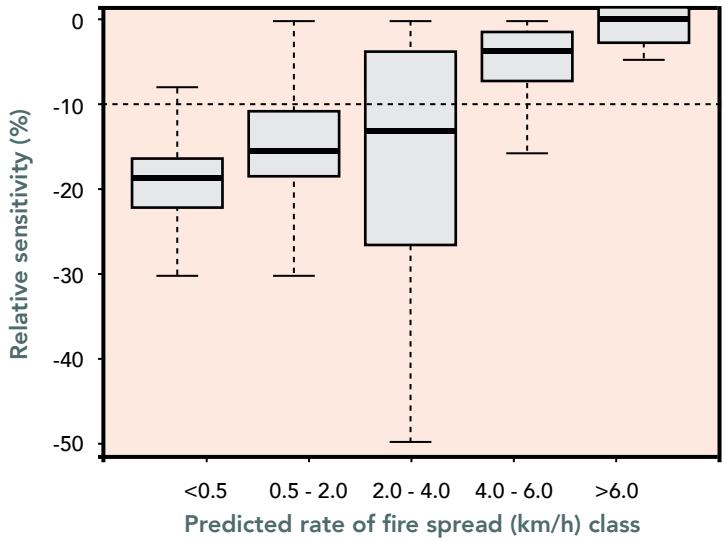

Figure 14. Distribution of relative sensitivity of the Vesta Mk 2 model to a 10% change in the fine dead fuel moisture content input as a function the predicted rate of fire spread grouped into 5 classes. Solid line in each box indicates the median. Each box defines the interquartile range. The solid horizontal lines outside each box show the maximum and minimum values (excluding outliers). The dashed horizontal line indicates a sensitivity equal to that of the change in the input value.

4.3 Fuel availability

Fuel availability typically refers to the proportion of potential fuel that is available for combustion in a given fire environment. In the context of fire spread modelling in Australia, fuel availability refers typically to fine fuels, both dead and live, although under extreme dryness conditions fuels other than fine can also contribute to flaming combustion.

There are a number of different fuel components within a fuel complex that go through a seasonal drying trend. Live vegetation such as grasses and shrubs, deeper organic litter layers and coarse woody debris are all fuels that show a relatively slow seasonal drying trend as a fire season progresses and general landscape dryness increases (Figure 15).

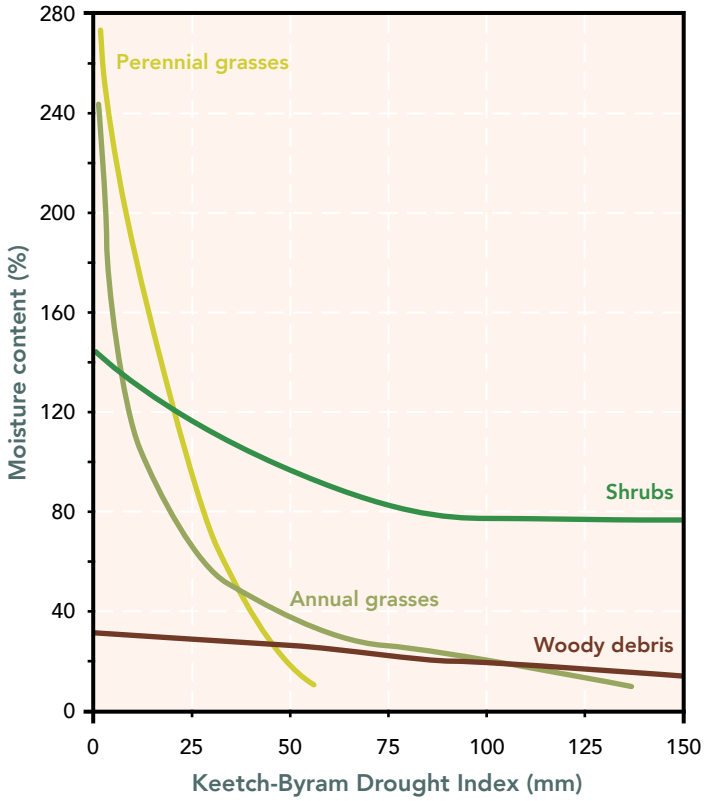

Figure 15. Drying trends of various common fuel components related to the Keetch-Byram Drought Index (Keetch and Byram 1968). Data from Canberra, ACT for November 1964 - March 1965 (based on illustration from Luke and McArthur 1978, p. 43).

Although the direct linkages between the moisture content of these fuels and the spread rate of fires have not been clearly established, it is generally recognised that as the moisture contents of these fuels decrease due to seasonal dryness, a higher proportion of all fuels become available for combustion, and in turn contribute to increases in fire spread rates and fireline intensity (McArthur 1966). Simultaneously, as a fire season progresses and more fuels become available to combust, areas that would normally not sustain fire propagation, such as creek lines, gullies or other sheltered areas within wet and rain forests, will increasingly be able to support active fire propagation.

In the Vesta Mk 2 model changes in fuel availability as landscape dryness increases is approximated by a sub-model linking the McArthur (1967) Drought Factor (*DF*) and the fuel availability fraction (which varies between 0 and 1) as described in Figure 16. This function implies that all fine fuel is available for combustion when the *DF* reaches its maximum value of 10.

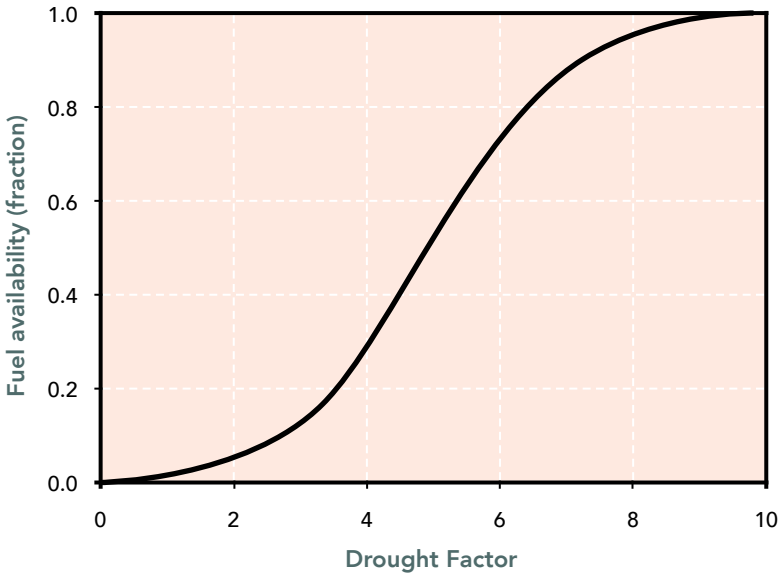

Figure 16. Relationship between the McArthur (1967) Forest Fire Danger Meter Drought Factor and fuel availability as used in Vesta Mk 2 model.

The use of a fuel availability function based on McArthur's *DF* is a pragmatic solution that enables an approximation of the effect of long-term rainfall deficit on landscape scale fuel availability for the purpose of operational fire spread prediction.

This approach works well for the prediction of the spread of large-scale fires in dry eucalypt forests, but it is recognised that it will have limitations for some specific applications, burning conditions and fuel types. The method is not able to reflect localised fuel availability, such as when aspect and slope have a marked effect on fuel drying. Similarly, its application to tall, multi-strata forests, such as denser wet eucalypt forests and temperate rainforests with enclosed microclimates, is expected to over-predict fuel availability, as understorey fine fuels in these forests may not have completely dried even when the *DF* has reached its maximum value of 10. For further refinement of the fuel availability function concept in these forest types see Section 7 – The special case of wet/tall forests.

The relative sensitivity of the model to changes in *DF* is illustrated in Figure 17. Overall, changes in the *DF* result in a smaller magnitude variation in the output than the input perturbation. The model shows higher sensitivity to the *DF* for the lower rate of fire spread classes, with a slightly wider distribution for the 2.0 to 4.0 km/h rate of fire spread class.

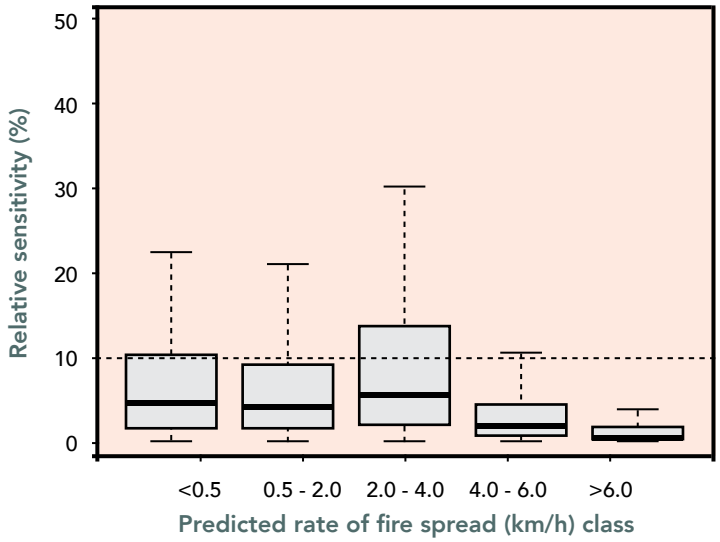

Figure 17. Distribution of relative sensitivity of the Vesta Mk 2 model to a 10% change in the Drought Factor input as a function the predicted rate of fire spread grouped into 5 classes. Solid line in each box indicates the median. Each box defines the interquartile range. The solid horizontal lines outside each box show the maximum and minimum values (excluding outliers). The dashed horizontal line indicates a sensitivity equal to that of the change in the input value.

4.4 Understorey fuel structure inputs

Some characteristics of fuel, the source of the energy driving a fire flame front, is a necessary input in fire spread models for eucalypt forests (*e.g.*, McArthur 1967). Understorey fuel properties are often correlated as they all allometrically evolve (or accumulate, if describing quantity) through time at comparable rates until they reach a steady state condition (Walker 1981). When explicitly incorporating one particular fuel parameter as an input into a fire spread model, this parameter is implicitly describing the effect of other correlated fuel properties into the model. Two understorey fuel characteristics are used in the Vesta Mk 2 model: the load of surface fine fuels (W_s; combining the load of the surface and near-surface fuel layers), and the average height of understorey near-surface and elevated fuels (h_u).

4.4.1 *Surface fuel load*

The amount of fine surface and near-surface fuels, henceforth referred to as *surface fuel load*, was chosen as a primary fuel structure input in the model due to its statistically significant influence on rate of fire spread and because it is a commonly assessed variable in fuel inventory studies in Australia (Figure 18). A wealth of information exists on its characterisation, relationships with vegetation, or fuel, types and modelling of accumulation over time.

Methods to estimate surface fuel load are not described in this report. Information on surface fuel load dynamics, namely accumulation rates, steady state condition and quantity in relation to time since last fire is generally already available to fire behaviour analysts in most jurisdictions across Australia. It is expected that users of the Vesta Mk 2 model will have access to this information before undertaking predictions of fire spread. Care should be taken to ensure that the value used as an input into the rate of fire spread model incorporates the load of both surface **and** near-surface fuel layers.

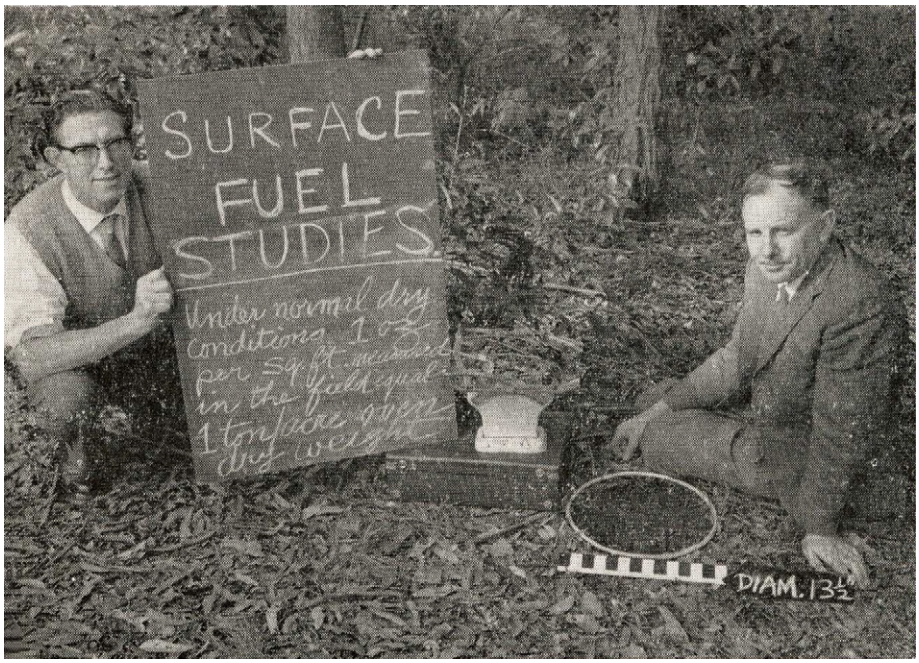

Figure 18. Estimating the surface fuel load in a dry eucalypt forest. Historical photo of Alan McArthur (left) and Harry Luke (right) circa 1960 (from McArthur and Luke 1963).

The effect of surface fuel load on the Vesta Mk 2 model varies with the phase dominating fire propagation and other environmental conditions. Surface fuel load is an input in the Phase I and II spread rate models. For low intensity fires spreading in Phase I, the effect is almost linear with a doubling in surface fuel load approximately doubling rate of fire spread. As fire intensity increases and the fuel strata dominating the heat transfer processes change, the effect of surface fuel load in the fire spread equation diminishes. For example, as the rate of spread of a fire spreading in Phase II increases, and its likelihood of transitioning to Phase III also increases, the effect of surface fuel load decreases.

Apart from the direct effect of surface fuel load on the fire spread equations of Phases I and II, surface fuel load also affects the likelihood of a fire transitioning from Phase I into Phase II. The effect of surface fuel load on rate of fire spread is thus not linear, but dynamic, with the magnitude of its effect depending on the fuel load itself and associated burning conditions. Figure 19 illustrates this dynamic where it is observed that a greater effect of fuel load is found when this quantity is more limiting (*e.g.*, <10 t/ha). In this range, an increase in surface fuel load can serve as a catalyst to escalate fire behaviour into the next spread phase with a significant increase in rate of fire spread. As shown in Figure 19, as the surface fuel load increases above 12.5 t/ha, it contributes to more moderate changes in rate of fire spread (Figure 19).

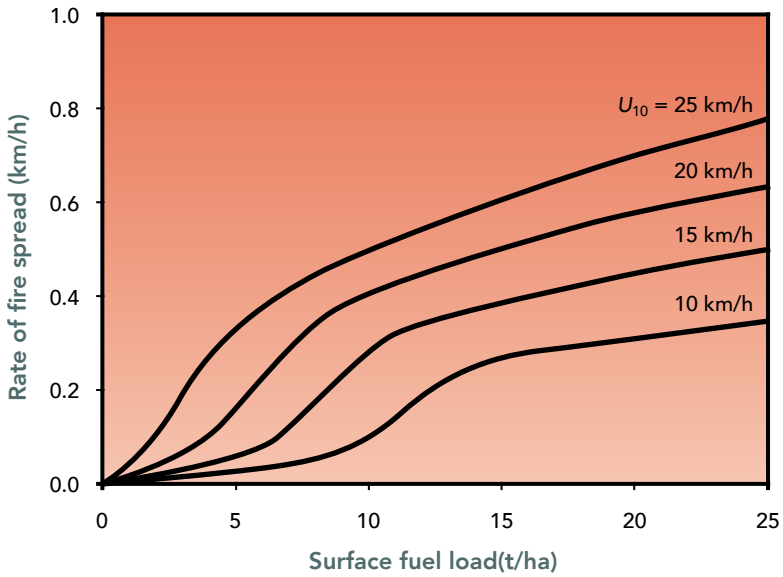

Figure 19. The effect of surface fuel load (quantity of fine fuel in the surface and near-surface layers) on the fire spread rate in Vesta Mk 2 model for four 10-m open wind speeds (U_{10}). Simulations are based on *MC* = 7%, h_u = 0.5 m, slope steepness = 0°, *WAF* = 3.3, and *DF* = 10.

The Vesta Mk 2 model has a moderate sensitivity to surface fuel load, with a percent change in the input resulting in a lower percent variation in the model output (Figure 20). The effect of fuel load is greater for slower propagating fires. For fires spreading with an *R* <2.0 km/h, a doubling of fuel load (100% increase) will result in a 50% increase in rate of fire spread. As the predicted rate of spread increases above 2 km/h, the effect of surface fuel load on the model output becomes negligible.

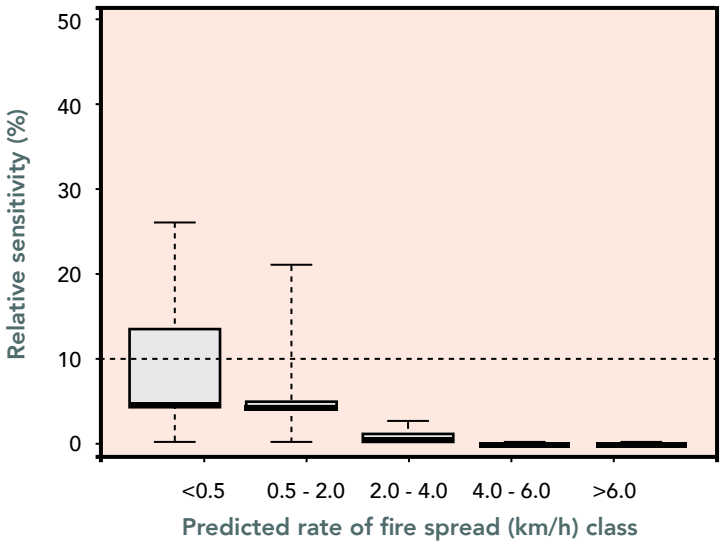

Figure 20. Distribution of relative sensitivity of the Vesta Mk 2 model to a 10% change in the surface fuel load input as a function of the predicted rate of fire spread grouped into 5 classes. Solid line in each box indicates the median. Each box defines the interquartile range. The solid horizontal lines outside each box show the maximum and minimum values (excluding outliers). The dashed horizontal line indicates a sensitivity equal to that of the change in the input value.

4.4.2 Understorey fuel height

The average height of understorey fuels was found to be an influential fuel characteristic affecting the spread rate of moderate- to high-intensity Phase II fires. This variable was defined as the average height of both the near-surface and elevated fuels weighted by their cover on a per area basis. This metric quantifies the volume of understorey fuels per unit area.

In the absence of direct measurements of average understorey fuel height, or the availability of near-surface and elevated fuel height and cover data from which the average understorey fuel height could be calculated, there is a need to estimate this variable from other available fuel descriptors. Given the existence of equations that estimate the fuel hazard scores / ratings and fuel heights for the elevated fuel layers for forest types across different states, predictive equations for understorey fuel height that rely on currently available fuel information were developed.

The best equation to predict the average understorey height (h_u, m) as a function of these other fuel attributes is:

$$h_u = -0.1 + 0.06\ FHS_{el} + 0.48\ h_{el} \quad [1]$$

where FHS_{el} and h_{el} are the elevated Fuel Hazard Score (0-4) and elevated layer height (m), respectively. Sample results for a discrete range of inputs are given in Table 4. These results can be used as a first approximation of understorey fuel height in the absence of on-site measurements.

In forest types where an elevated or tall shrub understorey is absent, the height of understorey fuel layer can be directly estimated from the average height of the near-surface fuel layer. Care should be taken to ensure the input is in meters, and not in centimetres as used in the original Vesta model.

Table 4. Understorey fuel height (m) derived from elevated layer Fuel Hazard Score and height

Height (m)	Fuel hazard score							
	0.5	1.0	1.5	2.0	2.5	3.0	3.5	4.0
0.25	0.05	0.08	0.11	0.14	0.17	0.2	0.23	0.25
0.5	0.17	0.2	0.23	0.26	0.29	0.32	0.35	0.38
0.75	0.29	0.32	0.35	0.38	0.41	0.44	0.47	0.5
1.0	0.41	0.44	0.47	0.5	0.53	0.56	0.59	0.62
1.25	0.53	0.56	0.59	0.62	0.65	0.68	0.71	0.74
1.5	0.65	0.68	0.71	0.74	0.77	0.8	0.83	0.86
2.0	0.89	0.92	0.95	0.98	1.01	1.04	1.07	1.1
2.5	1.13	1.16	1.19	1.22	1.25	1.28	1.31	1.34
3.0	1.37	1.4	1.43	1.46	1.49	1.52	1.55	1.58

Understorey fuel height has a smaller and less dynamic effect on fire spread rate predictions than surface fuel load, as it is only used in modelling Phase II fire spread. Figure 21 illustrates the effect of this variable for different burning conditions. The results show the effect of understorey fuel height to be more pronounced for lower height values (*e.g.*, <0.5 m) and the effect to decrease as height increases.

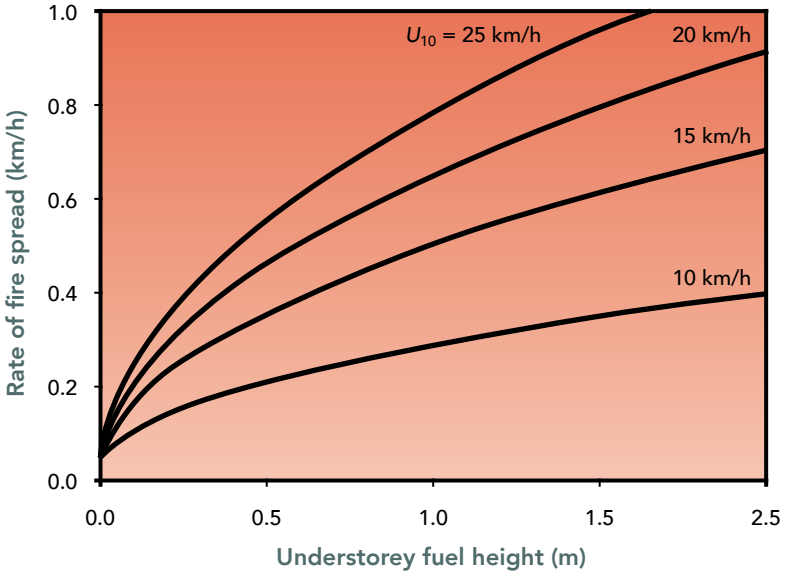

Figure 21. The effect of understorey fuel height in the Vesta Mk 2 model for four 10-m open wind speeds (U_{10}). Simulations are based on *MC* = 7%, W_s = 12 t/ha, slope steepness = 0°, *WAF* = 3.3, and *DF* = 10.

The Vesta Mk 2 model has a moderate to low sensitivity to changes in understorey fuel height (Figure 22), with the sensitivity to this input dependent on the dominating fire propagating phase. The effect is stronger for fires spreading with an R <2.0 km/h. Up to this level, a 10% increase in the input leads to an increase in the output of 4 to 6%. A doubling in understorey fuel height would result in about a 50% increase in rate of spread for fires propagating in Phase II (Figure 22). The effect of understorey fuel height diminishes considerably for burning conditions that lead to spread rates faster than 2.0 km/h, with the effect being negligible for fires spreading faster than 4.0 km/h.

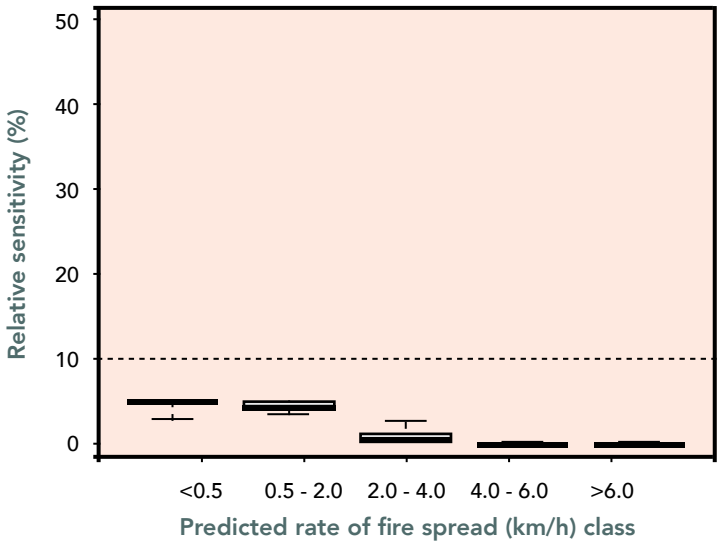

Figure 22. Distribution of relative sensitivity of the Vesta Mk 2 model to a 10% change in the understorey fuel height input as a function of the predicted rate of fire spread grouped into 5 classes. Solid line in each box indicates the median. Each box defines the interquartile range. The solid horizontal lines outside each box show the maximum and minimum values (excluding outliers). The dashed horizontal line indicates a sensitivity equal to that of the change in the input value.

The analysis of surface fuel load and understorey fuel height effects on the rates of fire spread presented above considers the variation in the fuel inputs independently, although it is expected that their dynamics will be correlated to a certain degree (*e.g.*, an increase in fuel load through time in a particular forest type will also be associated with an increase in understorey fuel height). Taking into account a more dynamic approach to fuel complex changes through time, Figure 23 presents an example of the potential fire spread for a dry eucalypt forest as a function of wind speed for four fuel ages (1-, 4-, 8- and 16-year old fuels measured as time since last fire), where both fuel load and understorey fuel height increase with time. The model identifies changes in fire spread that are more significant between the younger fuel ages, with the magnitude of the changes diminishing as fuels become older. This is most observable in the lower range of fire propagation, *e.g.*, wind speeds up to 20 km/h. Considering the full range of rate of fire spread, the figure also shows that the differences between fuel ages decrease as the rates of fire spread and intensity increases. For the low level of 7% fine dead fuel moisture content applied here, the differences in predicted rate of spread between ages 4- and 16-year-old fuels decrease considerably as wind speed increases above 30 km/h; under extreme fire spread potential conditions the effect of fuel structure has been found to diminish. The model is able to identify that for the 1-year-old fuels, characterised by low available surface fuel load and incipient understorey vegetation, the occurrence of Phase II and III fires is unlikely, and a fire will be limited to Phase I spread regardless of the severity of the burning conditions.

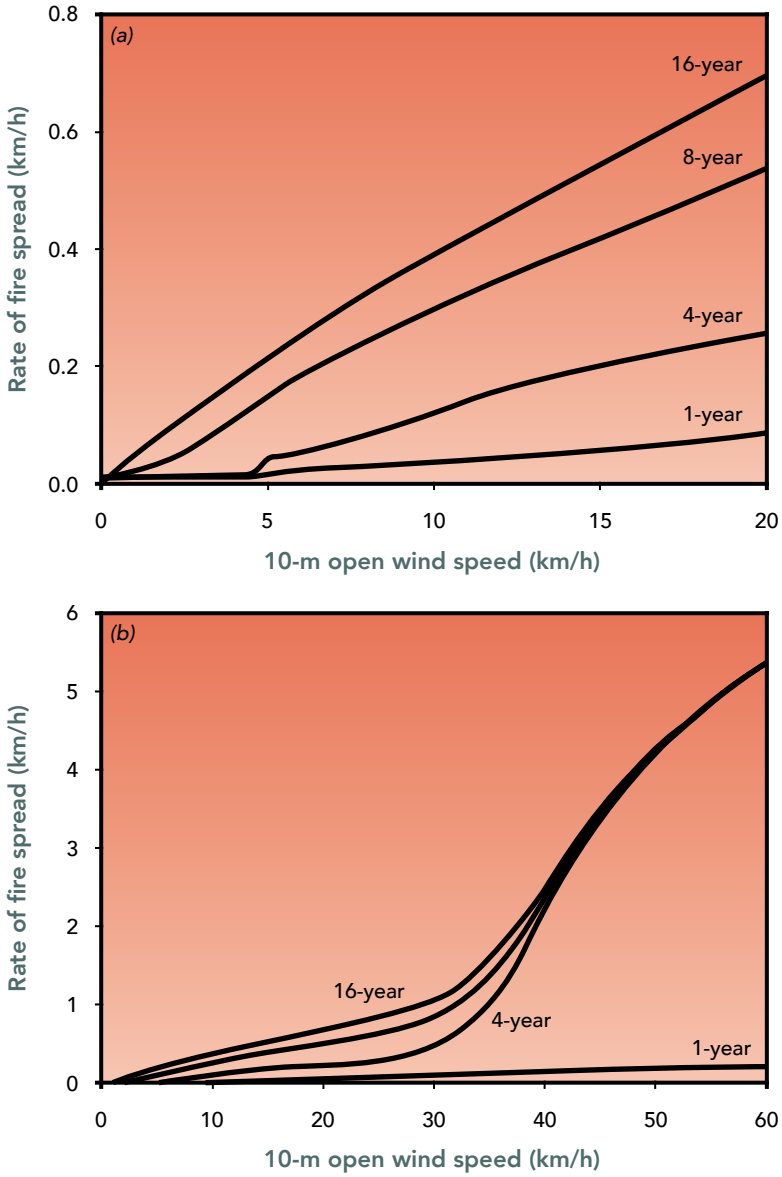

Figure 23. Modelled rate of fire spread in eucalypt forests based on the Vesta Mk 2 model as a function of wind speed and time since fire, (*a*) detail for low wind speeds; (*b*) over a broad wind speed range. Fuel characteristics are: for 1-year-old fuels - W_s = 2 t/ha and h_u = 0.05 m, for 4-year-old fuels - W_s = 8 t/ha and h_u = 0.11 m, for 8-year-old fuels - W_s = 13.5 t/ha and h_u = 0.29 m, for 16-year-old fuels - W_s = 16 t/ha and h_u = 0.45 m. Simulations based on *MC* = 7%, slope steepness = 0°, *WAF* = 2.5, and *DF* = 10.

4.5 Slope steepness

Slope steepness is a variable that has a dramatic effect on fire propagation. Fires spreading up slopes aligned with the wind are known to increase their rate of spread several fold compared to fire spread on flat ground. A.G. McArthur suggested a slope effect rule of thumb where the upslope rate of fire spread doubles for every 10° increase in slope steepness (Figure 24). This slope effect is intended to describe not only the mechanical effect of slope steepness on fire propagation, but also incorporate the broad topographic convergence and interactions associated with terrain in an open environment (*i.e.*, increased wind speed near ridge tops, drier fuels, etc.).

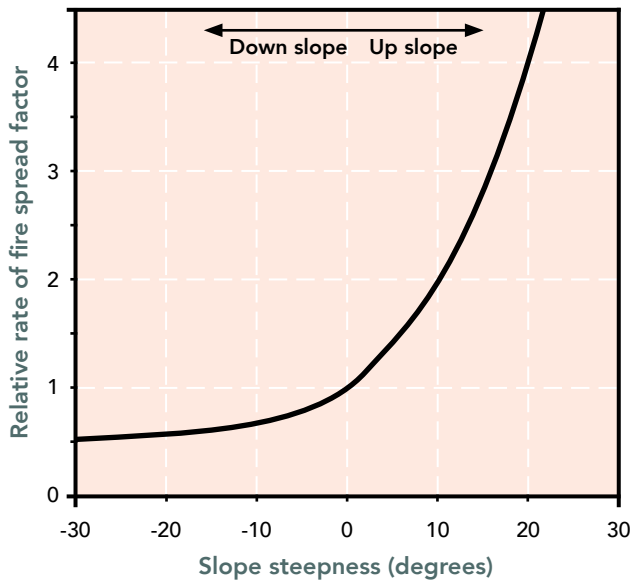

Figure 24. The effect of slope steepness on the rate of fire spread, for both McArthur (1967) upslope (slope > 0°) and Sullivan *et al.* (2014) downslope (slope < 0°) spread where the wind is aligned with the slope.

For the prediction of fire spread downslope, a corresponding decrease in rate of spread is expected, albeit not as strong as the upslope effect (Figure 24). Recent work suggests that the negative slope correction factor should not be less than half the flat ground rate of fire spread (Sullivan *et al.* 2014).

The appropriate use of the slope adjustments in operational fire spread predictions requires a judicious understanding of the local conditions influencing the spreading fire. McArthur's (1967) suggested his rule of thumb was most applicable to fires burning under milder conditions or still going through the build-up stage. For large wildfires burning across multiple drainages, particularly when spotting is occurring, the effect of slope steepness on the overall rate of fire spread may be regarded as negligible based on fire size considerations and the assumption that increases and decreases in rate of spread over positive and negative slopes will cancel each other out (Sullivan *et al.* 2014).

5 Spotting

Spotting, or the process of the transport of firebrands and the ignition of new fires outside the main active fire perimeter (Figure 25), is a complex, poorly understood and quantified phenomenon. Spotting is an inherent feature of wildfires spreading in eucalypt forests (Luke and McArthur 1978). Under certain environmental conditions spotting can be the dominant propagation mechanism driving high rates of fire spread (Cheney and Bary 1969).

Box 3. Spotting in eucalypt forests

Spotting is an important fire propagation process in high intensity fires in eucalypt forests. The type of tree bark will determine the size, shape and number of firebrands which, along with the prevailing fire behaviour and weather conditions will dictate the spotting distances and density of ignitions.

Fibrous bark, present in species such as *Eucalyptus obliqua* (Stringybark), *E. marginata* (Jarrah) and *E. macrorrhyncha* (Red stringybark), is easily ignited and dislodged from the trunk allowing simultaneously for vertical fire propagation into the overstorey and profuse short- to medium-range spot fire ignitions. Species with smooth decorticating bark (*e.g., E. viminalis* (Manna gum), *E. globulus* (Bluegum), *E. delegatensis* (Alpine ash)) provide aerodynamically efficient, firebrand material that can remain alight for long periods and be transported over considerable distances.

Spotting can be classified into three categories based on distance and density distribution.

Short-range spotting

Short-distance spotting (including ember showers) includes all spotfires up to 0.75 km from a fire front and is generally the result of embers and firebrands blown directly ahead of the fire with little to no lofting. Short-range spotting density tends to decrease with distance from the fire front. Greater spotting densities are expected under drier and windier burning conditions as litter fuels are more susceptible to ignition from smaller embers and more firebrands are transported in flatter trajectories.

The coalescence of multiple short-range spotfires results in the development of deep flaming zones, crowning and further generation and transport of burning embers. McArthur (1967) describes this process as key to how a fire maintains overall rates of spread much higher than expected in the absence of spotting. Key components for the maintenance of this process are the presence of high surface fuel loads, long unburnt eucalypt forest with a significant number of species with fibrous bark, high wind speeds and low fuel moisture contents. With fuel moisture contents <4% and in the presence of wind, the likelihood of spotfire ignitions increase significantly as the heat requirements for ignition are reduced. In this situation even tiny glowing particles have sufficient energy to start new spot fires.

Spotting, either short- (up to ≈0.75 km by Australian standards) or medium-range (up to ≈5 km) (Box 3), was present in the data used to develop the Vesta Mk 2 model and, hence, its effect in the model is implicitly accounted for in its formulation. As such, predictions by the model incorporate the nominal effects of short to medium spotting distances on the forward rate of fire spread where propagation of the fire front is not hindered in any way.

Longer spotting distances (*i.e.*, >5 km) occur under more severe fire weather conditions in most Australian eucalypt forests (McArthur, 1969; Rawson *et al.*, 1983; Storey *et al.*, 2020), but is more likely in gum or ribbon bark types where the bark can burn for long enough to traverse large distances and still successfully ignite a spot fire. The model does not implicitly

Medium-range spotting

Medium-distance spotting (1.0-5.0 km) results from embers and firebrands that are lofted briefly in the convection column, blown directly out of tree tops from an elevated position such as a ridge without being lofted or fall from the collapse of the convection column at a break in fuel or topography. In the absence of any break in fuel or topography, isolated medium-range spot fires are generally overrun by the main fire front. When a pattern of concentrated medium range spotting develops, pseudo flame fronts formed by coalescence of spot fires can lead to an immediate large increase of the overall rate of fire spread. Concentrated medium range spotting can produce mass fire or firestorm effects (Luke and McArthur 1978). In this situation a large number of coalescing fires causes strong turbulent inflow circulation that results in high intensity burning.

Long-range spotting

Long-distance spotting (>5 km) results from extended flight paths associated with significant lofting of firebrands in a well-developed convection column and long burn-out times. This class of spotting generally creates isolated ignitions that develop as a separate, independent fires. Long-range spotting of approximately 30 km has been authenticated on several occasions in eucalypt forests (Hodgson 1967; McArthur 1969; Cruz *et al.* 2012).

The firebrands responsible for long-range spotting are thought to be long streamers of decorticating bark that normally hang from the upper branches in certain smooth-barked eucalypt species such as *E. viminalis, E. globulus, E. delegatensis*. The bark strips curl into hollow tubes that when ignited at one end can burn for as long as 40 minutes. The long combustion times coupled with their good aerodynamic properties (*i.e.*, very low terminal velocity) allows these firebrands to be a viable ignition source even when transported over long distances. Long-range spotting also requires an intense fire that maintains a strong upward motion in the buoyant plume to transport relatively large fuel particles several kilometres above the ground and strong winds aloft to transport firebrands for extended distances downwind.

(Adapted from *A guide to rate of fire spread models for Australian vegetation*, 2015)

incorporate the effect of long-range spotting in its rate of spread predictions. The influence of these longer spotting distances on a wildfire's overall propagation rate is unclear. For a newly ignited spot fire occurring ahead of a wildfire to spread independently and result in an increased rate of spread relative to the model expectation, it will need to land in an area where wind flow is not constrained by the convection column. Spot fires initiating within the plume wake zone of a fire often spread without a general direction due to the light and variable winds within this region. These spot fires will likely be overrun by the main fire front and not increase its overall speed. The extent and width of this plume wake region, for any given combination of fire size and energy release rate, environmental conditions, or associated fire-atmosphere interactions, is presently unclear. As a result, the spotting distance that will result in a long-range spot fire growing independently of the main fire and increasing the overall propagation speed of the wildfire beyond that predicted by the Vesta Mk 2 model is unknown. Depending on the size and intensity of the fire, this could be 10-15 km ahead of the main advancing headfire. The occurrence of such long-range spot fires spreading independently of the main fire can lead to under-predictions when using the Vesta Mk 2 model. Users need to be aware of this limitation in the model.

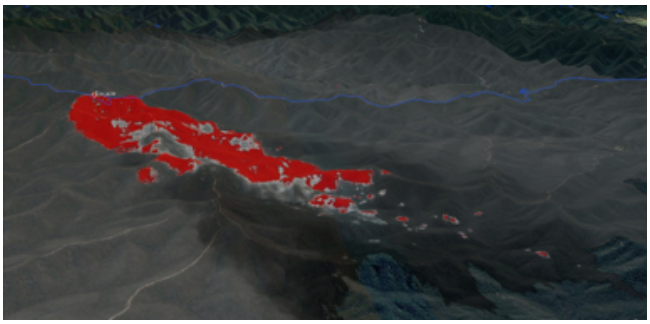

Figure 25. View of the Tambo 35 fire in Victoria during the early stages of the 30th December 2019 afternoon run. (above) Photograph taken of the fire at 15:39 approximately 1 hr after the fire run started (photo by Dale Appleton, DELWP). (left) Concurrent draped 3D linescan image at 15:34 showing extensive spotting ahead of the main fire, with maximum spotting distances up to 8 km (image courtesy of Owen Salkin).

6 Main model assumptions and limitations

The Vesta Mk 2 model is intended for the operational prediction of wildfire propagation in eucalypt forests over a broad range of fire spread rates and fireline intensities. The model is to be seen as a guide to potential fire spread rate. The prediction of fire spread and associated behaviour is both an art and science, combining the use of science-based fire spread models with incident-tailored fire weather forecasts and the experience of trained users with knowledge of landscape factors and fire dynamics processes that are not explicitly accounted in the models.

The use of the Vesta Mk 2 model should be underpinned by an awareness of its assumptions and limitations. The main assumptions can be summarised as:

- The model assumes a pseudo-steady state has been achieved, *i.e.*, the fire being predicted has already completed its build-up stage where the fire has accelerated from a point ignition to a steady-state rate of spread consistent with the prevailing burning conditions.
- The model aims to predict fire spread over time scales of one or more hours, based on the mean observed or forecasted weather conditions. The longer the time scale, the more accurate the predictions tend to be. The application of the model to short fire spread periods (*e.g.*, less than 30 minutes) is likely not to accurately reflect the finer scale variability in observed fire behaviour, such as the stalls and surges in propagation that occur in response to environmental changes (such as wind gusts and lulls) and fire-atmosphere interactions.
- Fuel structure influences are incorporated through inclusion of surface fuel load and understorey fuel height. Fuel characteristics are often correlated, and the effect of other fuel characteristics (*e.g.*, bark type and quantity, litter cover, shrub fuel load) is implicit in the effect described by these two fuel structure input variables.
- The effect of fine dead fuel moisture content assumes a homogenously dry litter and near-surface fuel layers as expected to occur under dry, summer-time conditions. Judicious use of realistic fuel moisture conditions under wetter scenarios (*e.g.*, after night-time dew formation or incipient rainfall) is required to produce better predictions of potential fire spread. Whenever possible, direct measurements of fine dead fuel moisture content should be made to validate and calibrate the predictions of the fuel moisture model.
- The effect of live fuel moisture content, either from understorey fuels or over-storey canopy fuels, and dead fuels other than fine, on the spread rate of a fire is implicitly accounted in the fuel availability fraction as inferred from the Drought Factor.

- The effect of long-term dryness and recent rainfall in affecting the fuel quantity contributing to fire propagation is approximated through the fuel availability fraction. This approach works well for the prediction of large-scale fire spread in dry eucalypt forests, but it is recognised that it will have limitations for some specific applications, burning conditions and fuel types.
- The effect of stand structure on the understorey wind speed is assumed to be described by simple wind adjustment factors *(WAF)*.
- The bulk effect of slope on rate of fire spread is as described by A.G. McArthur's rule of thumb in which rate of fire spread doubles the flat ground speed for every 10° slope steepness for upslope runs. The Kataburn model (Sullivan *et al*. 2014) is applicable for downslope runs.
- The effect of the occurrence of short- and medium-range spot fires (*e.g.*, <5 km) on the overall forward rate of fire spread is implicitly accounted for in the model.
- The model does not consider the effect of the occurrence of concentrated medium range spot fire ignitions that can lead to mass fire or firestorm effects. Occurrence of this type of spotting behaviour is expected to cause under-predictions in fire propagation and possibly should be modelled separately.
- The model does not incorporate the effect of long-range spotting (*e.g.*, >5 km). The occurrence of this kind of spot fire occurrence can, in certain cases, lead to under-predictions of fire propagation.
- Given the inherent variability and uncertainty in the estimation of environmental conditions and fire behaviour in wildfire situations, expect a margin of error in rate of fire spread of at least ±40% (*e.g.*, a predicted rate of spread of 3.0 km/h will imply a range of 1.8-4.2 km/h in possible rate of spread).

The model does not incorporate fire spread dynamics resulting from significant changes in wind direction such as those associated with the passage of cold fronts, or sea breezes, over the fire area. The process that converts a fire's flank into a broad head fire is complex and presently poorly understood, with the growth in fire area in the hours immediately following the frontal passage typically unrelated to the factors that typically drive fire behaviour such as wind strength and the relative humidity of the associated air mass (McArthur 1967; Rawson *et al*. 1983). The unquantified effects of fire-atmosphere interactions on the precision of model predictions also remain unclear.

7 The special case of wet/tall forests

Wet eucalypt forests (also, often called tall eucalypt forests) are structurally distinct from the typical dry eucalypt forest that predominates across much of Australia's forested regions. Growing in wetter and richer soil substrates, these forests are characterised by a dense over- and understorey canopy layer, high annual fuel accumulation rates and a moist microclimate (Cawson *et al.* 2020; Pickering *et al.* 2021). The relatively deep soil and surface fuel layers, and the dense understorey allow for a large amount of moisture to be stored in the system. This creates a within-forest environment with higher average moisture contents and an overall lower fuel availability than observed in dry eucalypt forests under the same general climatic and weather influences. A wet eucalypt forest will typically require long periods of drying before fuels become available to burn. The dense overstorey and understorey canopy strata of wet forests also significantly impact the within-stand wind flow, with these winds being typically lower than those observed in contiguous dry open forests.

These differences make wet forests less prone to support fire ignition and active fire propagation when compared with dry forests. It is worth noting that high intensity fire propagation can still occur in wet forests during extreme fire potential periods associated with prolonged drought.

The Vesta Mk 2 model can be applied to wet eucalypt forests, contingent upon minor adaptations to capture the specific fire environment of these forests, namely: (1) fine dead fuel moisture content is accurately estimated; (2) the Drought Factor and fuel availability calculation are representative of a wet forest environment; and (3) an appropriate *WAF* is chosen.

7.1 Fine dead fuel moisture content

The estimation of fine dead fuel moisture content from forecasted weather data for fire behaviour prediction in wet eucalypt forests needs to consider two important factors: (1) the differences between forecasted weather conditions and the conditions at the fuel level; and (2) moisture fluxes from the soil and deep litter profile into the surface litter and near-surface fuel layers. These will vary with environmental conditions, landscape position (namely aspect) and seasonal dryness throughout a fire season (Slijepcevic *et al.* 2018; Pickering *et al.* 2021). The moisture content of the top of the surface fuel layer in a wet forest can be 2-5% moisture content points higher than that found in a dry forest under the same atmospheric conditions (Pickering *et al.* 2021). In the absence of an adequate model parameterisation to estimate fine dead fuel moisture content in wet forests, the assessment of this variable *in situ* through direct measurement combined with forecast weather data is likely to produce the most accurate estimation of its value. In the absence of direct measurements, Table M2 for nighttime fuel moisture content in Section 10 can be seen as a first approximation. Use of this table in wet forests should rely on fuel level air temperature and relative humidity measurements or estimates.

7.2 Drought Factor / fuel availability

Rainfall deficit and its effect in reducing the moisture content of different fuel components, such as live grass and shrubs, deep organic layers and coarse woody debris, has been identified as one of the most influential factors affecting the likelihood a fire will ignite and actively spread in a wet forest (Cawson *et al.* 2020). The absence of rainfall during extended periods will reduce the moisture in the soil – litter interface and the overall moisture in the system. This leads to an increase in the fraction of the total fuel available that can potentially contribute to flaming combustion. The Vesta Mk 2 parameterisation described in the present guide (Section 4.3) considers a Drought Factor – fuel availability relationship developed for dry eucalypt forests. In wet eucalypt forests this relationship is expected to be different due to a number of factors, namely the denser overstorey and moister under-storey micro-climate.

For wildfire prediction operations in wet forests, it is suggested that fuel availability be estimated from an adjusted Drought Factor that accounts for the effect of (1) stand structure on understorey drying processes and (2) slope and aspect in exposing or sheltering fuels to solar radiation. This adjusted Drought Factor, described in Duff *et al.* (2018) and given in Eqs. 5 - 7 in Section 9 of this guide, was idealised by Kevin Tolhurst and is implemented in Phoenix RapidFire version 5.0 (Tolhurst *et al.* 2008).

Figure 26a illustrates how the adjusted Drought Factor for a wet eucalypt forest (*WAF* = 5; south-eastern facing slope) differs during the 2019/20 fire season (data from Canberra Airport AWS) from the original McArthur (1967) Drought Factor typically applied to a dry eucalypt forest. The two trends, with the *DF* for the dry forest reaching a maximum of 10 in late December and the adjusted *DF* for a wet forest reaching a maximum value of approximately 7 later in the fire season, illustrate the differences in the likely understorey fuel dryness and associated fuel availability (Figure 26b), between the two forest types. While not yet formally evaluated against field data, in the interim the adjusted *DF* for wet forests is deemed applicable for landscape wildfire spread prediction purposes.

7.3 Wind adjustment factor

The application of the Vesta Mk 2 model to wet forest types in a wildfire prediction situation requires a judicious assessment of the most appropriate wind adjustment factor (*WAF*) based on the topographic location of the forest, the forest structure and the open wind speed itself. Table 3 provides a simplified range of *WAF* for dry and wet forests, although it should be recognised that wet forests are often located in sheltered locations and the most appropriate *WAF* can be higher than the values prescribed. The values of *WAF* for wet forests in Table 3, between 5 and 6.5, may be seen as conservative. This ensures the risk of under-prediction in a high intensity wildfire propagation scenario is reduced. But users should be aware that higher values, up to 10, are likely to be representative of certain stands (Moon *et al.* 2019), namely ones with a denser mid- and understorey canopy layer and located in sheltered conditions (*e.g.*, lower in a narrow valley).

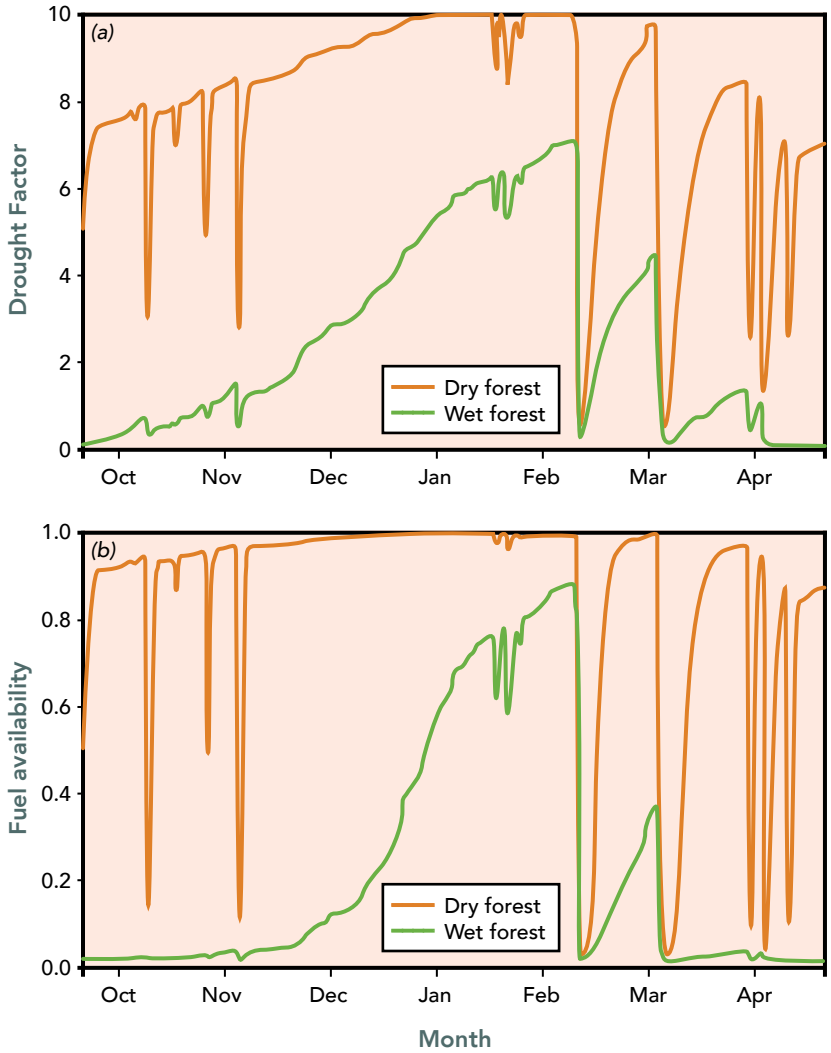

Figure 26. Seasonal variation in (a) Drought Factor and (b) fuel availability for dry (original McArthur (1967) method, brown) and wet (adjusted as per Duff *et al.* (2018), green) eucalypt forest for the summer 2019/20 in Canberra. Wet forest calculations assume a *WAF* of 5 and a south-eastern facing slope).

Box 4. Dry vs Wet forests – capturing differences in fire spread potential

The differences in fire spread potential between dry and wet forests (Figure 27) change as the fire season progresses and with the daily variation in burning conditions. The differences diminish with an increase in general landscape dryness and severity of the burning conditions. Figure 28 presents the differences in predicted fire spread rate for dry and wet forests for the 2019/20 fire season on the (a) North Black Range fire and (b) Orroral Valley fire on days in which these fires spread under heightened fire spread potential. The North Black Range fire occurred early in the fire season when its area was characterised by a *DF* of 9 and a KBDI of 84 mm. In contrast, the Orroral Valley fire occurred later in the season under an area *DF* of 10 and a KBDI of 150 mm.

Figure 27. Contrasting understorey structures for a dry (top) and wet (bottom) eucalypt forests.

The results show the Vesta Mk 2 model, with adjustments for Drought Factor, fine dead fuel moisture content and wind adjustment factor, highlights substantial differences in the predicted rate of fire spread for the two fuel types earlier in the season, when the moister conditions in the wet forests limited the amount of fuel available for combustion. The predicted rate of spread in the dry forests at this time was three to four times higher than in the wet forests during the afternoon peak burning period. As the fire season progressed and landscape dryness increased, the Vesta Mk 2 model outputs suggest the differences in predicted fire spread rate to decrease. In late January the dry forest predictions were approximately only two to three times greater than the wet forest scenario during the afternoon.

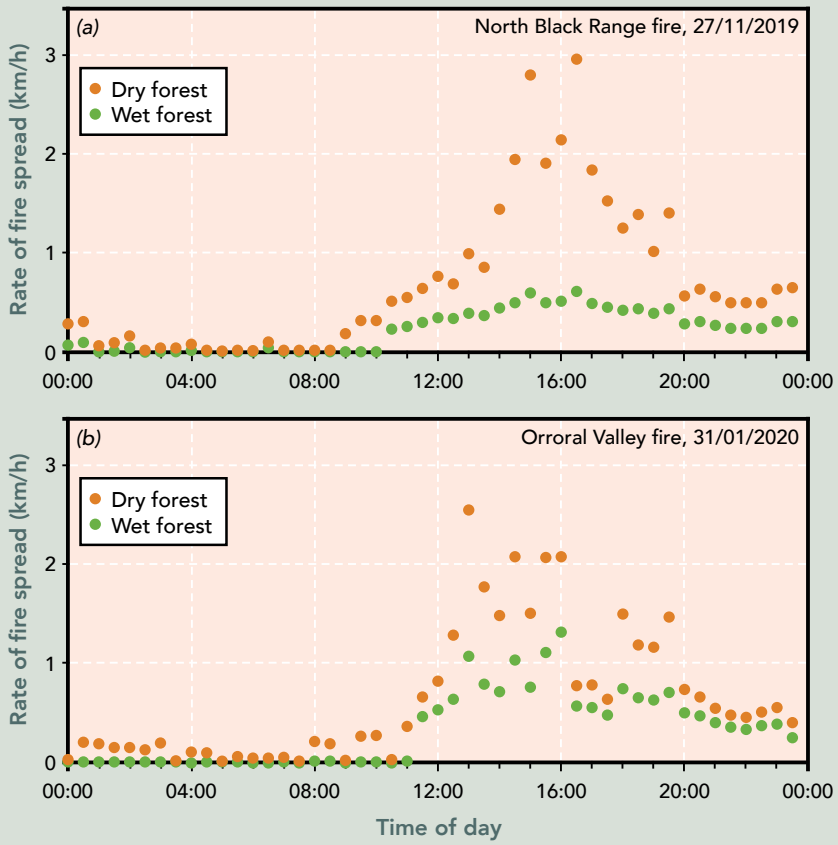

Figure 28. Differences in predicted rate of fire spread for dry and wet forest conditions for (*a*) the North Black Range fire on 27/11/2019; and (*b*) the Orroral Valley fire on 31/01/2020. Simulations based on Canberra AWS (within 40 km of each fire) observations. Wet forest inputs: W_s = 19 t/ha, h_u = 0.9 m and *WAF* = 5. Dry forest inputs: W_s = 12 t/ha, h_u = 0.6 m and *WAF* = 3. Simulations assume level topography.

8 Model evaluation and accuracy

The Vesta Mk 2 model has been evaluated against a number of independent datasets comprising moderate intensity experimental fires (n = 14) and well-documented wildfires of varying intensity in eucalypt forests of southern Australia (n = 90). Rates of fire spread in these datasets ranged between 0.20 and 8.0 km/h. Mean absolute error produced by the model against the experimental fire data was 0.13 km/h, or 39% of the observed rate of spread, with no noticeable bias. For the wildfire dataset, where the simulations are affected by a larger uncertainty in model inputs, the mean absolute error was 1.3 km/h or 84% when considering error on a relative basis. For the wildfire dataset the model predictions had an overall over-prediction bias of 0.25 km/h, or about 20% of the mean error. This level of error is consistent with, although lower than, the results obtained with other empirically-based fire spread models evaluated against wildfire data (Cruz and Alexander 2013).

Figure 29 shows the distribution of error with observed rate of fire spread for the wildfire evaluation data. The results show the percent error to decrease as observed rates of fire spread increase, suggesting that the model works best for the conditions in which it is most critical. Highest percent errors were observed for fires spreading slower than 2.0 km/h, with fires spreading above this threshold having absolute percent errors less than 30%. The results also show that the model tended to over-predict the spread rate of fires observed to spread slower than 4 km/h, and on average under-predicted fires spreading above this threshold. For this latter class of f*ires*, the average error was below 25% of the observed rate of fire spread.

It is worth emphasising that the level of error obtained for the wildfire dataset is to a degree a function of the uncertainties and inaccuracy of the inputs used to run the model against wildfire data. This evaluation against the wildfire data was based on coarse general environmental information (*e.g.*, fuel, wind speed, etc.) believed to be representative of the fire run duration, although high uncertainty exists. No adjustments were made to the data to take into account local understanding of conditions that might influence the assumed model inputs (*e.g.*, knowledge of wind channelling phenomena in the headfire run area might lead to a correction of the wind speed measured at the nearest weather station).

It is believed that during operational situations, fire behaviour analysts will have access to further information that can help reduce prediction errors. These sources of data include using fine-scale incident weather forecasts and other fine tuning of inputs based on local knowledge of fuels, local weather patterns and antecedent fire behaviour. As such, it is believed that in an operational fire prediction scenario, qualified and experienced fire behaviour analysts will be able to produce more accurate predictions than reported here.

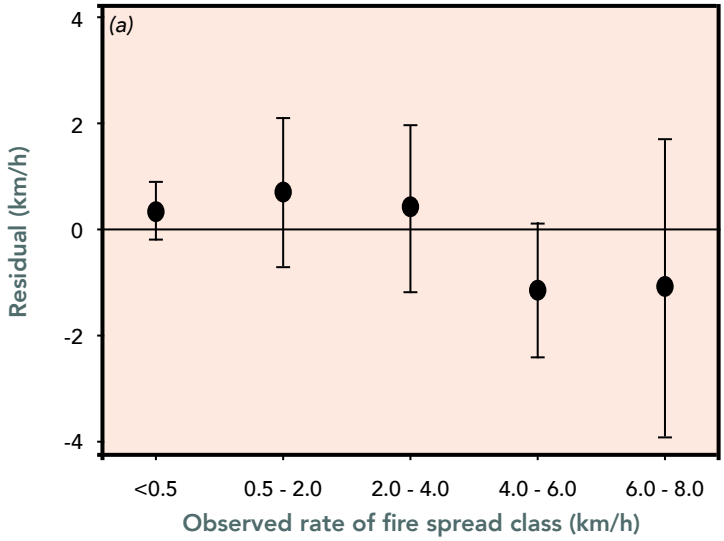

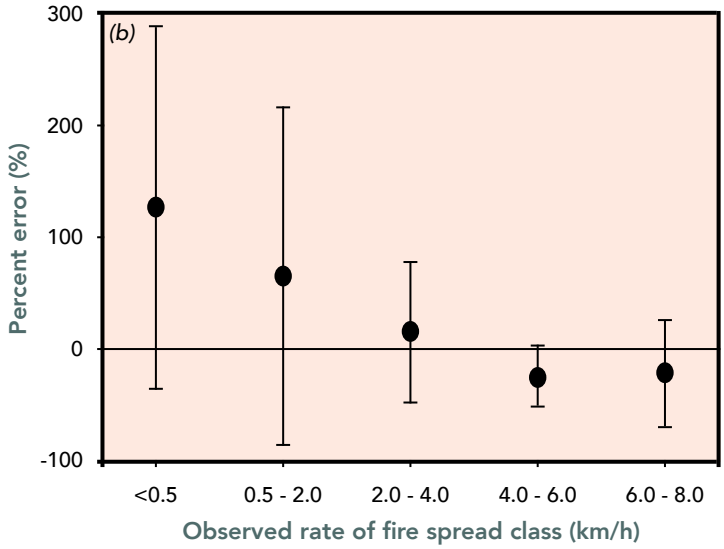

Figure 29. Summary of model performance by observed rate of fire spread class. (*a*) Mean and standard deviation of residuals (difference between predicted and observed rates of spread). (*b*) Mean and standard deviation of the prediction error as a percentage.

Box 5. Fire spread prediction error - operational implications

As simulations of fire spread models are used to support decision making during a wildfire event, it is important to understand the effect of uncertainty in fire spread predictions, either due to errors associated with inaccurate inputs or limitations of the model itself. What is the impact of a 50% under- or over-prediction error? A decision maker will need to understand the uncertainty and potential bias associated with the fire spread predictions to better use fire simulations to support decision-making and tailor the actions to be taken.

Figure 30 summarises the impact of a rate of spread prediction error on a hypothetical example of a wildfire starting 6.0 km upwind of a community. The example assumes that 0.5 h after ignition the wildfire is spreading at 3.0 km/h. For the sake of simplicity, the wildfire is assumed to have been detected the moment immediately after ignition and that in the early stages of fire propagation (*i.e.*, during its build-up phase), the fire was spreading at the pseudo steady-state rate of spread. The example considers the wildfire to impact the community 2.0 h after ignition, a fire behaviour analyst produced a forecast of fire spread 0.5 h after the ignition was detected (1.5 h before impact), and local authorities would act upon the forecast to immediately release a warning to the general public.

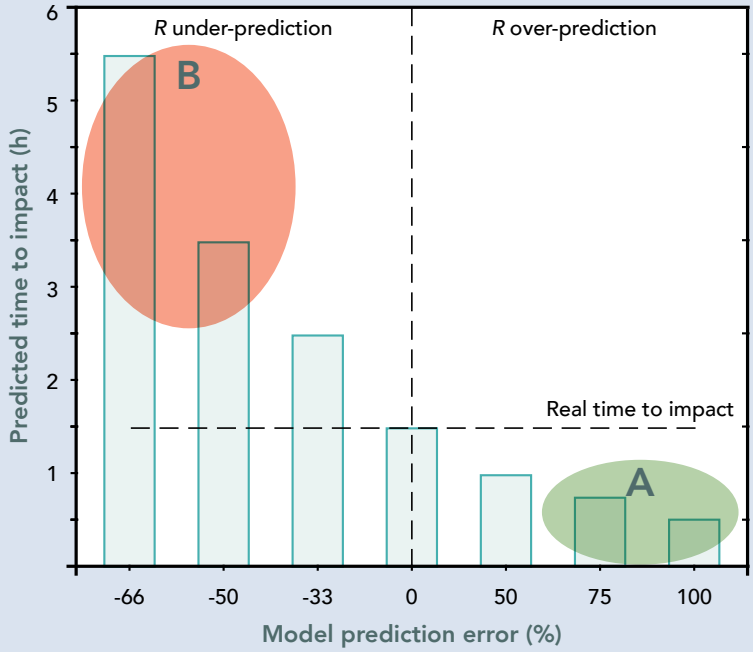

Figure 30. Effect of fire spread model prediction percent error in the predicted time to impact for a hypothetical wildfire impacting a community 1.5 h after a real-time fire behaviour prediction is completed. A (rate of spread over-prediction) and B (rate of spread under-prediction) are regions where the magnitude of the error can result in negative impacts on the decision making (from Cruz *et al.* 2020).

If a correct rate of fire spread prediction of 3.0 km/h is made (*i.e.*, 0% error) and an evacuation warning is issued, then the population has 1.5 h to act before the wildfire impacts the community. An over-prediction in fire spread rate will result in a reduction in the perceived time to impact (*i.e.*, the community will think that they have less time to act than in reality). As the over-prediction in rate of fire spread increases, the predicted time to impact will decrease to a level that might lead to a negative outcome (area A in Figure 29 – *e.g.*, emergency services decide that the time for the community to safely evacuate is too short and thus do not issue an evacuation warning). This is most apparent for a 100% over-prediction error (a rate of fire spread prediction of 6.0 km/h), where a predicted time to impact of 0.5 h might lead to a change from evacuation to a "shelter-in-place" warning. Such advice against evacuation when in reality time would allow for its safe implementation can potentially put members of the general public at undue risk.

Similarly, under-prediction biases of wildfire rate of spread can also have a detrimental, but different, impact on the decision-making process. Under-predictions will result in an erroneous over-estimation of the time to fire impact, potentially removing the necessary sense of urgency (area B in Figure 30). For example, the largest under-prediction in Figure 30 suggesting 6.0 h to impact might delay any warnings to the general public during a critical time period. Considering 1.0 h as a time scale relevant for community evacuation, prediction errors up to 33% are not likely to have a detrimental impact on public safety. However, it is errors above this threshold, and in particular under-prediction errors, that can result in a lack of timely and appropriate warnings that will lead to the most detrimental consequences.

Albini (1976) pointed out that there are three principal reasons for disagreement between model predictions and observed fire behaviour, no matter which models are being used:

1. The model may not be applicable to the situation.
2. The model's inherent accuracy may be at fault.
3. The data used in the model may be inaccurate.

While much progress has been made in wildland fire behaviour research over the past 45 years or so since the publication of his seminal work on fire behaviour modelling, these same three basic principles still remain valid to this day.

9 Equations and calculation procedures

The calculation of fire spread rate in the Vesta Mk 2 model follows a number of intermediate steps. The model has seven core inputs (Table 2):

- 10-m open wind speed (U_{10});
- a wind adjustment factor (*WAF*) that converts 10-m open wind speed (U_{10}) into understorey, eye-level or 2-m height wind speed (U_2);
- the moisture content of fine dead fuels (*MC*);
- Drought Factor (*DF*);
- the load of surface and near-surface fuels (W_s);
- understorey fuel height (h_u); and
- slope steepness (θ).

Table 5 below summarises the various steps involved into calculating the forward rate of fire spread from these inputs. Figure 31 provides a graphical workflow for the operation of the Vesta Mk 2 model.

Table 5. Vesta Mk 2 calculation steps with input variables highlighted in bold

Step	Calculation	Inputs	Output	Equation
1	Within stand wind speed	$\boldsymbol{U_{10}}$ and ***WAF***	U_2	2
2	Fine dead fuel moisture effect	***MC***	ΦM_d	3
3	Fuel availability	***DF***	ΦFA	4
4	Fuel moisture effect	ΦM_d and ΦFA	ΦM	8
5	Likelihood of Phase II and III	$\boldsymbol{U_{10}}$, U_2, ΦM, $\boldsymbol{W_s}$	P(II), P(III)	9, 10, 11, 12
6	Slope effect	$\boldsymbol{\theta}$	$\Phi\theta$	13
7	Rate of fire spread of Phase I, II and III	$\boldsymbol{U_{10}}$, U_2, ΦM, $\boldsymbol{W_s}$, $\boldsymbol{h_u}$, $\Phi\theta$	R(I), R(II), R(III)	14, 15, 16
8	Forward rate of fire spread	P(II), P(III), R(I), R(II), R(III)	R	17

Step 1: Within stand wind speed

Considering U_{10} as the benchmark forecast wind speed with which to make a wildfire spread prediction, the understorey wind speed, U_2, can be estimated from the appropriate wind adjustment factor (*WAF*; Table 3) that take into account forest cover and height:

$$U_2 = \frac{U_{10}}{WAF} \quad [2]$$

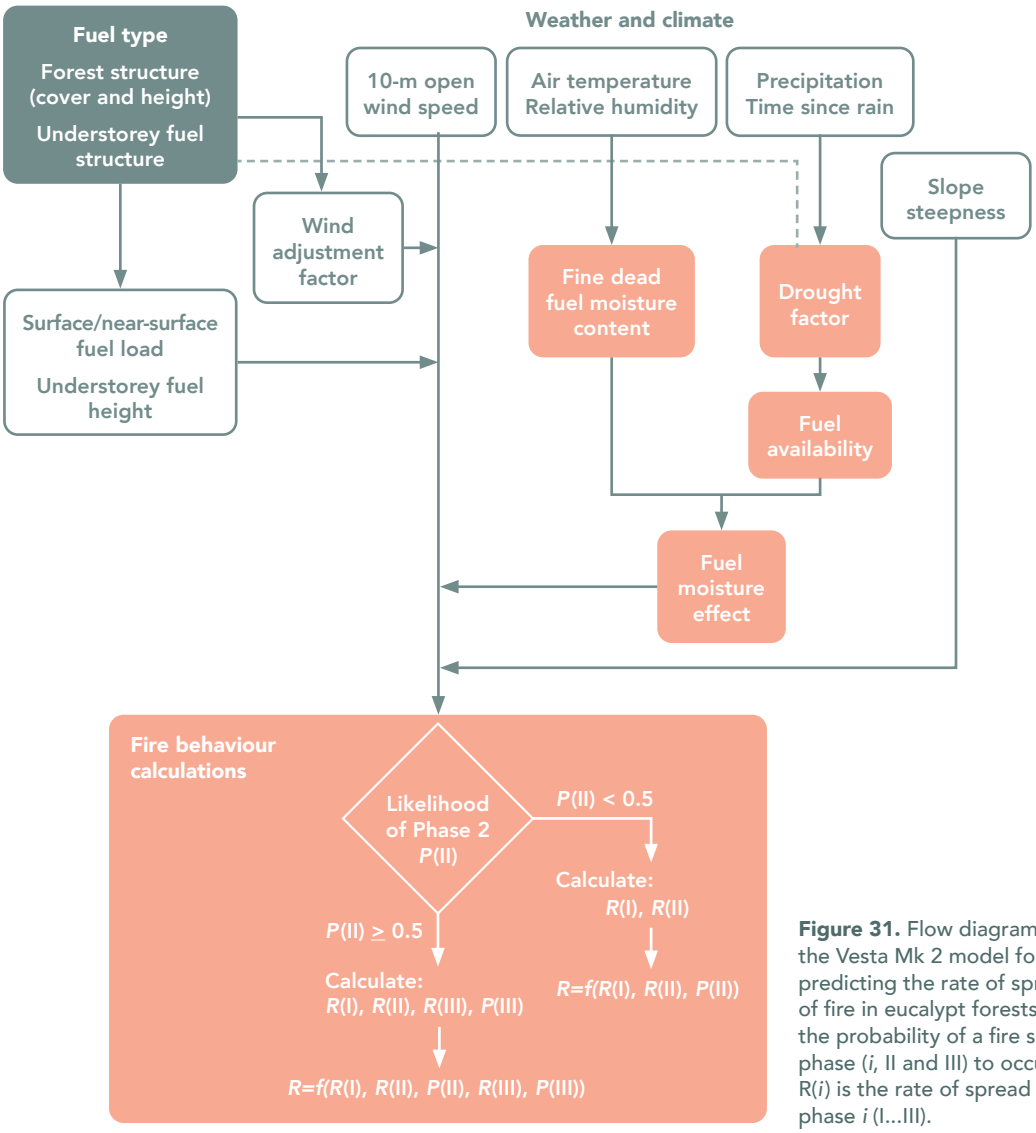

Figure 31. Flow diagram of the Vesta Mk 2 model for predicting the rate of spread of fire in eucalypt forests. P(*i*) is the probability of a fire spread phase (*i*, II and III) to occur. R(*i*) is the rate of spread for phase *i* (I...III).

Step 2: Fine dead fuel moisture content effect

The effect of fine dead fuel moisture content on rate of fire spread employs a function that produces a factor (ΦM_d) varying between 0 (fire extinguishment) obtained for moisture content (*MC*) values above 24% (moisture content of extinction), and 1.0, attained when the *MC* is 4.1% or less:

$$\Phi M_d = \begin{cases} 1, & \text{if } MC \leq 4.1\% \\ 0.9082 + 0.1206\ MC - 0.03106\ MC^2 + 0.001853\ MC^3 - 0.00003467\ MC^4, & \text{if } 4.1\% < MC \leq 24\% \\ 0, & \text{if } MC > 24.0\% \end{cases} \quad [3]$$

Step 3: Fuel availability

The effect of long-term dryness in increasing fuel availability (*FA*) for combustion and fire spread potential is incorporated through a fuel availability function (ΦFA) calculated from the McArthur (1967) Drought Factor:

$$\Phi FA = \frac{1.008}{1 + 104.9\ exp(-0.9306\ DF)} \quad [4]$$

where ΦFA varies between 0 and 1.0, and *DF* is the McArthur Drought Factor. The *DF* is provided in Bureau of Meteorology weather forecasts or can be calculated separately.

For the special case of wet forests, an adjusted *DF* (DF_{wet}) that takes into account stand structure, KBDI (Keetch-Byram Drought Index; Keetch and Byram 1968) and aspect should be used in lieu of the standard *DF*. DF_{wet} considers two adjustments. The first adjustment (C1) takes into account *KBDI* and *WAF* as a proxy of stand structure (Duff *et al.* 2018):

$$C1 = (0.0046\ WAF^2 - 0.0079\ WAF - 0.0175)\ KBDI + (-0.9167\ WAF^2 + 1.5833\ WAF + 13.5) \quad [5]$$

with *WAF* restricted to vary between 3 and 5.

The second adjustment (C2) takes into account topographic aspect for areas with a slope steepness ≥ 10°. For the case of wet forests, this adjustment should be applied to aspects between 90° (east) and 225° (south-west). C2 is calculated as:

$$C2 = -0.000000002204\ \alpha^4 + 0.000000995\ \alpha^3 + 0.00006335\ \alpha^2 - 0.04895\ \alpha + 1.8 \quad [6]$$

where α is the azimuth or aspect. If slope steepness < 10°, C2 = 0.

The adjusted *DF* for wet forests is then given by:

$$DF_{wet} = \mathrm{DF}\left(\frac{max(C1+C2,0)}{10}\right) \quad [7]$$

with DF_{wet} being constrained between 0 and 10.

The Drought Factor – fuel availability relationship described here is applicable for landscape fire spread prediction. For other applications, such as prescribed burning, it is not believed the *DF* metric has the resolution and the spatial detail to accurately describe the proportion of fuels available to burn in specific landscape locations. Fuel availability estimated from measured surface and profile moisture content is likely to better represent the amount of fuel contributing to fire propagation. But that is a story to be told in a different place.

Step 4: Fuel moisture effect

The effect of fine dead fuel moisture content factor (ΦM_d; Step 2) and long-term fuel dryness (ΦFA; Step 3) are combined into an overall fuel moisture effect function (ΦM):

$$\Phi M = \Phi M_d \, \Phi FA \quad [8]$$

After Step 4, calculations focus on fire behaviour components, namely the likelihood of fire spreading within a phase, the rate of spread associated with each phase and the overall rate of fire spread.

Step 5: Probability of transition between phases

The likelihood of a fire transitioning from Phase I to Phase II was modelled through logistic regression analysis. In the absence of fire spread data in incipient fuel beds, as expected to describe a recently burnt area, a constrain was imposed in the transition probability to ensure model outputs are consistent with expectations when fire is spreading where fuel quantity and structure limits the energy available to cause vertical fire transitions. A two-step equation is used to calculate the probability of the fire transitioning from Phase I into Phase II (P(*II*)):

$$\mathrm{P(II)} = \begin{cases} 0 & \text{if } W_s < 1.0 \text{ t/ha} \\ 1/(1 + exp(-g(x))) & \text{if } W_s \geq 1.0 \text{ t/ha} \end{cases} \quad [9]$$

with 1.0 t/ha being arbitrarily selected as the threshold value below which a transition into Phase II is not possible. The function $g(x)$ is the logit for the transition likelihood that takes into account the effect of understorey wind speed (U_2), the fuel moisture effect (ΦM) and fuel load (W_s, t/ha) of surface fuels:

$$g(x) = -23.9315 + 1.7033\, U_2 + 12.0822\, \Phi M + 0.95236\, W_s \quad [10]$$

Modelling the likelihood that a fire will transition from Phase II to Phase III follows a similar approach. As with the Phase II transition, there was no data available to investigate the effect of the understorey fuel structure on the transition from Phase II into Phase III when the fuel structure state limits this transition. To ensure the model does not identify Phase III fire propagation if understorey fire activity does not generate enough energy to initiate the transition, a Phase II rate of fire spread constraint was applied. This constrain states that if the Phase II rate of fire spread is below 0.3 km/h the likelihood of fire spread to Phase III is nil. The two-step model for the probability of a fire transitioning to Phase III (P(III)) takes into account this rule and a logistic model for transition likelihood:

$$P(III) = \begin{cases} 0 & \text{if } R(II) < 0.3 \text{ km/h} \\ 1/(1 + exp(-g(x))) & \text{if } R(II) \geq 0.3 \text{ km/h} \end{cases} \quad [11]$$

The logit for the onset of Phase III ($g(x)$) incorporates the effect of U_{10} and ΦM:

$$g(x) = -32.3074 + 0.2951\ U_{10} + 26.8734\ \Phi M \quad [12]$$

Step 6: Slope effect

The slope function relies on A.G. McArthur slope effect rule of thumb for upslope fires and the Kataburn down slope effect refinement from Sullivan *et al.* (2014):

$$\Phi\theta = \begin{cases} 2^{\left(\frac{\theta}{10}\right)} & \text{if } \theta > 0 \\ \dfrac{2^{(-\theta/10)}}{2\,(2^{(-\theta/10)}) - 1} & \text{if } \theta < 0 \end{cases} \quad [13]$$

with θ being the slope steepness in degrees.

Step 7: Rate of fire spread of Phase I, II and III

The Vesta Mk 2 model calculates the potential rate of spread (R) associated with each spread phase (Table 1). The propagation in each phase has different controls, hence distinct inputs and functional forms.

The model for R in Phase I (*i.e.*, $R(I)$) was developed with the analysis of low- to moderate-intensity experimental fire data with an observed R up to 0.21 km/h. Non-linear regression analysis resulted in $R(I)$ estimated as:

$$R(I) = \left(0.03 + 0.05024\ (U_2 - 1)^{0.92628} \left(\frac{W_s}{10}\right)^{0.79928}\right)\ \Phi M\ \Phi\theta \quad [14a]$$

where U_2 is the understorey wind speed (km/h) at 2-m height in the forest, W_s is surface fuel load (t/ha) as defined in the present study, ΦM is the overall fuel moisture effect and $\Phi\theta$ the slope steepness effect.

Equation 14a is applicable for U_2 > 2 km/h. For lower wind speeds, R(I) is given by:

$$R(\mathrm{I}) = 0.03\ \Phi M\ \Phi\theta \qquad [14b]$$

The model for rate of fire spread within Phase II was developed with experimental fire data within an observed R range between 0.10 and 1.5 km/h. Through non-linear regression analysis the best model for $R(II)$ had U_2, two fuel structure variables, W_s and understorey height (h_U), plus ΦM and $\Phi\theta$:

$$R(\mathrm{II}) = 0.19591\,(U_2)^{0.8257} \left(\frac{W_s}{10}\right)^{0.4672} h_u^{0.495}\ \Phi M\ \Phi\theta \qquad [15]$$

The Phase III model for R was fitted with a subset of the data with R >1.0 km/h. The best model form was found to be:

$$R(\mathrm{III}) = 0.05235\,(U_{10})^{1.19128}\ \Phi M\ \Phi\theta \qquad [16]$$

Step 8: Forward rate of fire spread

The prediction of the overall R requires combining the output of the likelihood/probability of the phase transitions (Step 5) and the fire spread rate models for the various phases (Step 7). The likelihood models indicate which fire spread phase will dominate the overall fire spread calculation for a given set of weather and fuel conditions. The overall rate of fire spread output (R) is a sum of the value predicted by each of the R(i) models weighted by the likelihood of the fire spreading in that state (eq. 17):

$$R = \begin{cases} R(I)\ (1 - P(II)) + R(II)\ P(II) & \text{if } P(II) < 0.5 \\ (R(I)\ (1 - P(II)) + R(II)\ P(II))\ (1 - P(III)) + R(III)\ (P(III)) & \text{if } P(II) \geq 0.5 \end{cases} \qquad [17]$$

This formulation avoids the abrupt changes in R that would occur if a fixed transition threshold was used to indicate a change from a lower to a higher state (*e.g.*, using P(II) ≥0.5 (50%) to shift from $R(I)$ to $R(II)$), or the inverse).

10 Fire behaviour tables

The tables in this section enable the estimation of the rate of spread of fire in eucalypt forests using the Vesta Mk 2 model to be made without need for a computer. Associated flame height and fireline intensity can also be estimated. The tables are derived from the application of the full model presented in the previous section to six idealised dry eucalypt forest fuel conditions. The tabular results are based on a number of simplifying assumptions and should be seen as a first approximation of potential fire behaviour to be used as field reference. For more accurate model predictions users should rely on a computerized fire simulation software or application.

Use of the Fire behaviour tables:

1. Calculate **Fine dead fuel moisture content** using Tables M1 – M2 from forecasted or observed *air temperature, relative humidity, cloudiness* and *the time of day*.
2. Calculate **Fuel moisture effect** using Table Mef from ***Fine dead fuel moisture content*** (Tables M1 – M2, Step 1) and *Drought Factor.*
3. Select the target **Fuel condition** from Table F.
4. Calculate the **Rate of fire spread** (flat ground) using Tables R1 – R6 from ***Fuel moisture effect*** and *10-m open wind speed*. Use Table R1 to R3 for low productivity forests and Tables R4 to R6 for moderate productivity forests.
5. If **Slope steepness** is deemed influential at the location (see Section 4.5), adjust the ***Rate of fire spread*** by multiplying it by the **Slope relative effect** (Table S) using an estimate of the average *slope angle* (in degrees or percent) in the direction of the wind.
6. Estimate **Fireline intensity** from the Fire Behaviour Characteristics Chart (front inside cover) using slope-adjusted ***Rate of fire spread*** and *Fuel consumed*. Fuel consumed is an estimate of the fuel consumed in flaming combustion, which depending on the level of fire activity can incorporate surface, elevated, bark and canopy fuel layers.
7. Estimate **Flame height** (Table Fh) using slope-adjusted ***Rate of fire spread*** and *Elevated fuel height*.

Key:
Italics – direct input (measured or forecasted);
Bold – sub-model output;
Bold italic – input from previous sub-model output.

The fire spread prediction worksheet included in this guide can be used to record input data and fire spread calculations.

Fuel moisture content tables

Table M1

Daytime fine dead fuel moisture content (% oven-dry weight)

Relative humidity (%)	Clear sky, peak burning period[1]				Overcast sky, other daytime period			
	Air temperature (°C)				Air temperature (°C)			
	10	20	30	40	10	20	30	40
5	3.2	3.0	2.8	2.6	3.5	3.5	3.1	2.6
10	3.8	3.6	3.4	3.3	4.4	4.4	3.9	3.5
15	4.4	4.2	4.1	3.9	5.2	5.2	4.8	4.3
20	5.1	4.9	4.7	4.5	6.1	6.1	5.6	5.2
25	5.7	5.5	5.3	5.1	6.9	6.9	6.5	6.0
30	6.3	6.1	5.9	5.7	7.8	7.8	7.3	6.9
35	6.9	6.7	6.5	6.4	8.6	8.6	8.2	7.7
40	7.5	7.3	7.2	7.0	9.5	9.5	9.0	8.6
45	8.2	8.0	7.8	7.6	10.3	10.3	9.9	9.4
50	8.8	8.6	8.4	8.2	11.2	11.2	10.7	10.3
55	9.4	9.2	9.0	8.8	12.0	12.0	11.5	11.1
60	10.0	9.8	9.6	9.5	12.8	12.8	12.4	11.9
65	10.6	10.4	10.3	10.1	13.7	13.7	13.2	12.8
70	11.3	11.1	10.9	10.7	14.5	14.5	14.1	13.6
75	11.9	11.7	11.5	11.3	15.4	15.4	14.9	14.5

1 Applicable for clear sky conditions between October and March for the 12:00-17:00 period

Dark grey shaded cells are outside the bounds of validation data (source: Gould *et al*. 2007b)

Table M2

Nighttime fine dead fuel moisture content (% oven-dry weight)

Relative humidity (%)	Air temperature (°C)			
	10	20	30	40
10	4.1	4.1	3.6	3.1
15	5.1	5.1	4.6	4.1
20	6.1	6.1	5.6	5.1
25	7.1	7.1	6.6	6.1
30	8.1	8.1	7.6	7.1
35	9.0	9.0	8.6	8.1
40	10.0	10.0	9.6	9.1
45	11.0	11.0	10.5	10.1
50	12.0	12.0	11.5	11.0
55	13.0	13.0	12.5	12.0
60	14.0	14.0	13.5	13.0
65	15.0	15.0	14.5	14.0
70	16.0	16.0	15.5	15.0
75	17.0	17.0	16.5	16.0

Dark grey shaded cells are outside the bounds of validation data (source: Gould *et al.* 2007b)

Fuel moisture effect table

Table Mef

Fuel moisture effect

Fine dead fuel moisture content (%)	Drought Factor						
	4	5	6	7	8	9	10
4	0.29	0.50	0.72	0.87	0.95	0.98	1.00
5	0.27	0.48	0.68	0.82	0.90	0.93	0.94
6	0.25	0.44	0.63	0.76	0.83	0.86	0.87
7	0.22	0.39	0.57	0.68	0.74	0.77	0.78
8	0.20	0.35	0.50	0.60	0.66	0.68	0.69
9	0.17	0.30	0.43	0.52	0.57	0.59	0.60
10	0.15	0.26	0.37	0.45	0.49	0.51	0.51
11	0.12	0.22	0.31	0.38	0.41	0.43	0.43
12	0.10	0.18	0.26	0.32	0.35	0.36	0.37
13	0.09	0.16	0.22	0.27	0.29	0.30	0.31
14	0.07	0.13	0.19	0.23	0.25	0.26	0.26
15	0.06	0.11	0.16	0.20	0.22	0.22	0.23
16	0.06	0.10	0.15	0.18	0.19	0.20	0.20
17	0.05	0.10	0.14	0.17	0.18	0.19	0.19
18	0.05	0.09	0.13	0.16	0.17	0.18	0.18
19	0.05	0.09	0.13	0.16	0.17	0.18	0.18
20	0.05	0.09	0.13	0.15	0.16	0.17	0.17
21	0.05	0.08	0.12	0.14	0.15	0.16	0.16
22	0.04	0.07	0.10	0.12	0.13	0.14	0.14
23	0.03	0.05	0.07	0.08	0.09	0.09	0.09
24	0.01	0.01	0.02	0.02	0.02	0.02	0.03

Fuel condition

The fire spread rate tables consider fuel dynamics through time for two distinct dry eucalypt forests growing in different productivity sites: a low and a moderate productivity forest. The low productivity one is characteristic of a forest growing in a poor subtracts and annual precipitation below 700 mm. The moderate productivity forest is characteristic of areas with better soils and higher annual rainfall. For each forest type, the tables give predictions for three stages of fuel accumulation, for a total of 6 fuel structure situations (Table F). Users will need to select the most appropriate fuel condition by considering surface fuel accumulation, understorey fuel height and wind adjustment factor.

Table F

Standardised fuel structure for low and moderate productivity eucalypt forests

Fuel characteristics	Low productivity forest			Moderate productivity forest		
	4-year	8-yr	Long unburned	4-year	8-yr	Long unburned
Surface fuel load (t/ha)	7.0	11.5	14.0	7.6	14.3	16.8
Elevated fuel load (t/ha)	0.8	1.7	2.0	2.6	4.0	4.2
Bark fuel load (t/ha)	0.6	1.5	2.0	2.6	2.2	2.7
Total fuel load (t/ha)	8.4	14.7	18.0	12.8	20.5	23.7
Understorey fuel height (m)	0.2	0.4	0.5	0.65	0.9	1.1
Elevated fuel height (m)	0.3	0.6	0.8	1.1	1.5	1.8
Wind Adjustment factor		3.0			3.5	
Rate of Spread Table	R1	R2	R3	R4	R5	R6

Fire spread rates

Table R1

Rate of fire spread (km/h) for low productivity forest, young fuels (≈4-year-old)

Moisture content effect	10-m open wind speed (km/h)									
	5	10	15	20	25	30	35	40	45	50
0.3	0.01	0.03	0.05	0.07	0.11	0.15	0.17	0.19	0.21	0.23
0.35	0.01	0.04	0.06	0.08	0.14	0.17	0.20	0.22	0.24	0.27
0.4	0.01	0.05	0.07	0.10	0.16	0.20	0.23	0.25	0.28	0.31
0.45	0.01	0.05	0.08	0.12	0.19	0.22	0.26	0.29	0.32	0.35
0.5	0.02	0.06	0.09	0.15	0.21	0.25	0.28	0.32	0.36	0.42
0.55	0.02	0.06	0.10	0.17	0.23	0.28	0.31	0.36	0.42	0.57
0.6	0.02	0.07	0.11	0.20	0.26	0.30	0.35	0.41	0.55	1.01
0.65	0.02	0.07	0.13	0.22	0.28	0.33	0.39	0.52	0.93	1.98
0.7	0.02	0.08	0.15	0.24	0.30	0.37	0.48	0.84	1.79	3.13
0.75	0.02	0.09	0.18	0.26	0.34	0.44	0.74	1.60	2.89	3.90
0.8	0.02	0.10	0.20	0.28	0.39	0.65	1.39	2.61	3.64	4.35
0.85	0.03	0.11	0.22	0.34	0.55	1.18	2.31	3.33	4.07	4.68
0.9	0.03	0.13	0.24	0.45	0.96	1.98	2.98	3.74	4.37	4.97
0.95	0.03	0.15	0.26	0.76	1.63	2.59	3.36	4.01	4.63	5.25
1.0	0.04	0.17	0.28	1.28	2.17	2.93	3.59	4.23	4.88	5.53

Table results assume flat ground – see Table S for slope correction

Table R2

Rate of fire spread (km/h) for low productive forest, mature fuels (≈10-year-old)

Moisture content effect	10-m open wind speed (km/h)									
	5	10	15	20	25	30	35	40	45	50
0.3	0.01	0.05	0.09	0.18	0.23	0.27	0.30	0.34	0.37	0.41
0.35	0.01	0.06	0.12	0.21	0.27	0.31	0.35	0.39	0.44	0.48
0.4	0.01	0.07	0.16	0.25	0.31	0.36	0.40	0.45	0.50	0.54
0.45	0.01	0.08	0.19	0.28	0.34	0.40	0.45	0.51	0.56	0.62
0.5	0.02	0.10	0.23	0.32	0.38	0.44	0.51	0.57	0.63	0.71
0.55	0.02	0.12	0.26	0.35	0.42	0.49	0.56	0.63	0.71	0.88
0.6	0.02	0.15	0.29	0.38	0.46	0.53	0.61	0.70	0.86	1.30
0.65	0.03	0.18	0.32	0.41	0.50	0.58	0.68	0.83	1.22	2.18
0.7	0.04	0.22	0.35	0.45	0.54	0.64	0.78	1.13	2.01	3.23
0.75	0.06	0.25	0.37	0.48	0.58	0.72	1.03	1.81	2.99	3.93
0.8	0.08	0.27	0.40	0.52	0.65	0.92	1.61	2.72	3.68	4.36
0.85	0.10	0.30	0.43	0.57	0.81	1.39	2.42	3.37	4.08	4.68
0.9	0.13	0.32	0.47	0.68	1.17	2.09	3.02	3.75	4.37	4.97
0.95	0.16	0.35	0.54	0.95	1.74	2.63	3.37	4.01	4.63	5.25
1.0	0.18	0.39	0.72	1.39	2.21	2.94	3.60	4.24	4.88	5.53

Table results assume flat ground – see Table S for slope correction

Table R3

Rate of fire spread (km/h) for low productivity forest, long unburned fuels

Moisture content effect	10-m open wind speed (km/h)									
	5	10	15	20	25	30	35	40	45	50
0.3	0.01	0.07	0.17	0.23	0.28	0.33	0.37	0.41	0.46	0.50
0.35	0.01	0.09	0.20	0.27	0.33	0.38	0.43	0.48	0.53	0.58
0.4	0.02	0.12	0.24	0.31	0.37	0.44	0.49	0.55	0.61	0.67
0.45	0.02	0.15	0.27	0.35	0.42	0.49	0.56	0.62	0.69	0.75
0.5	0.03	0.19	0.30	0.39	0.47	0.54	0.62	0.69	0.77	0.86
0.55	0.05	0.22	0.34	0.43	0.52	0.60	0.68	0.76	0.86	1.04
0.6	0.07	0.25	0.37	0.47	0.56	0.65	0.75	0.85	1.02	1.45
0.65	0.09	0.28	0.40	0.51	0.61	0.71	0.82	0.98	1.37	2.28
0.7	0.12	0.30	0.43	0.55	0.66	0.78	0.93	1.28	2.11	3.27
0.75	0.15	0.33	0.46	0.59	0.71	0.87	1.18	1.92	3.04	3.95
0.8	0.18	0.35	0.49	0.63	0.79	1.06	1.72	2.78	3.69	4.37
0.85	0.20	0.37	0.53	0.69	0.94	1.50	2.47	3.39	4.09	4.69
0.9	0.21	0.40	0.57	0.80	1.27	2.15	3.04	3.75	4.37	4.97
0.95	0.23	0.42	0.64	1.04	1.80	2.66	3.37	4.01	4.63	5.25
1.0	0.25	0.47	0.80	1.44	2.24	2.95	3.60	4.24	4.88	5.53

Table results assume flat ground – see Table S for slope correction

Table R4

Rate of fire spread (km/h) for moderate productivity forest, young fuels (≈4-year-old)

Moisture content effect	10-m open wind speed (km/h)									
	5	10	15	20	25	30	35	40	45	50
0.3	0.01	0.03	0.05	0.06	0.11	0.22	0.28	0.31	0.34	0.38
0.35	0.01	0.04	0.05	0.08	0.15	0.27	0.32	0.36	0.40	0.44
0.4	0.01	0.04	0.06	0.10	0.20	0.32	0.37	0.42	0.46	0.50
0.45	0.01	0.05	0.07	0.12	0.26	0.36	0.42	0.47	0.52	0.57
0.5	0.02	0.05	0.08	0.16	0.31	0.41	0.47	0.52	0.58	0.66
0.55	0.02	0.06	0.09	0.20	0.36	0.45	0.51	0.58	0.66	0.83
0.6	0.02	0.06	0.11	0.25	0.41	0.49	0.56	0.65	0.80	1.25
0.65	0.02	0.07	0.13	0.31	0.45	0.54	0.62	0.77	1.17	2.15
0.7	0.02	0.08	0.17	0.36	0.49	0.59	0.73	1.08	1.97	3.21
0.75	0.02	0.09	0.21	0.41	0.54	0.67	0.98	1.77	2.97	3.93
0.8	0.03	0.10	0.26	0.46	0.61	0.87	1.57	2.70	3.67	4.36
0.85	0.03	0.12	0.32	0.52	0.76	1.35	2.40	3.37	4.08	4.68
0.9	0.03	0.15	0.38	0.63	1.13	2.07	3.02	3.75	4.37	4.97
0.95	0.04	0.19	0.48	0.91	1.72	2.63	3.36	4.01	4.63	5.25
1.0	0.05	0.28	0.68	1.37	2.21	2.94	3.60	4.24	4.88	5.53

Table results assume flat ground – see Table S for slope correction

Table R5

Rate of fire spread (km/h) for moderate productivity forest, mature fuels (≈10-year-old)

Moisture content effect	10-m open wind speed (km/h)									
	5	10	15	20	25	30	35	40	45	50
0.3	0.01	0.06	0.17	0.27	0.33	0.39	0.44	0.49	0.54	0.59
0.35	0.01	0.08	0.22	0.32	0.39	0.45	0.51	0.57	0.63	0.69
0.4	0.02	0.11	0.26	0.37	0.45	0.52	0.59	0.66	0.72	0.79
0.45	0.02	0.15	0.31	0.41	0.50	0.58	0.66	0.74	0.82	0.90
0.5	0.03	0.19	0.35	0.46	0.56	0.65	0.74	0.82	0.91	1.02
0.55	0.05	0.24	0.39	0.51	0.61	0.71	0.81	0.91	1.02	1.20
0.6	0.07	0.28	0.43	0.56	0.67	0.78	0.89	1.00	1.18	1.60
0.65	0.10	0.32	0.47	0.60	0.72	0.84	0.97	1.15	1.52	2.39
0.7	0.14	0.35	0.51	0.65	0.78	0.92	1.09	1.43	2.23	3.32
0.75	0.17	0.38	0.55	0.70	0.84	1.02	1.33	2.04	3.10	3.96
0.8	0.21	0.41	0.58	0.75	0.92	1.21	1.83	2.83	3.71	4.37
0.85	0.23	0.44	0.62	0.81	1.07	1.61	2.53	3.41	4.09	4.69
0.9	0.25	0.47	0.67	0.92	1.38	2.21	3.06	3.76	4.38	4.97
0.95	0.27	0.50	0.74	1.14	1.86	2.68	3.38	4.01	4.63	5.25
1.0	0.29	0.54	0.89	1.50	2.26	2.96	3.60	4.24	4.88	5.53

Table results assume flat ground – see Table S for slope correction

Table R6

Rate of fire spread (km/h) for moderate productivity forest, long unburned fuels

Moisture content effect	10-m open wind speed (km/h)									
	5	10	15	20	25	30	35	40	45	50
0.3	0.02	0.14	0.25	0.33	0.40	0.46	0.53	0.59	0.65	0.71
0.35	0.04	0.18	0.30	0.39	0.46	0.54	0.61	0.68	0.75	0.82
0.4	0.06	0.22	0.34	0.44	0.53	0.62	0.70	0.78	0.86	0.94
0.45	0.08	0.26	0.39	0.50	0.60	0.69	0.79	0.88	0.97	1.06
0.5	0.12	0.30	0.43	0.55	0.66	0.77	0.88	0.98	1.08	1.20
0.55	0.15	0.34	0.48	0.61	0.73	0.85	0.96	1.08	1.21	1.40
0.6	0.18	0.37	0.52	0.66	0.80	0.93	1.05	1.19	1.38	1.78
0.65	0.21	0.40	0.57	0.72	0.86	1.01	1.15	1.34	1.71	2.52
0.7	0.23	0.43	0.61	0.77	0.93	1.09	1.28	1.62	2.36	3.38
0.75	0.26	0.47	0.65	0.83	1.00	1.20	1.51	2.18	3.16	3.98
0.8	0.28	0.50	0.70	0.89	1.09	1.38	1.97	2.90	3.73	4.38
0.85	0.30	0.53	0.74	0.96	1.23	1.75	2.60	3.43	4.10	4.69
0.9	0.31	0.56	0.79	1.06	1.51	2.28	3.09	3.77	4.38	4.97
0.95	0.33	0.60	0.86	1.26	1.93	2.70	3.39	4.01	4.63	5.25
1.0	0.35	0.64	0.99	1.57	2.29	2.96	3.60	4.24	4.88	5.53

Table results assume flat ground – see Table S for slope correction

Slope correction

Table S

Relative effect of slope steepness on rate of fire spread

	Slope angle (°)	Slope gradient (%)	Relative effect
Upslope	20	36	4.0
	15	27	2.8
	12.5	22	2.4
	10	18	2.0
	7.5	13	1.7
	5	9	1.4
	2.5	4	1.2
	0	0	1.0
Downslope	-2.5	-4	0.9
	-5	-9	0.8
	-7.5	-13	0.7
	-10	-18	0.7
	-12.5	-22	0.6
	-15	-27	0.6
	-20	-36	0.6

Flame height

Table Fh

Flame height (m)

Rate of fire spread (km/h)	Elevated fuel height (m)				
	0.25	0.5	1.0	1.5	2.0
0.1	0.7	0.8	1.1	1.5	2.1
0.15	0.9	1.1	1.5	2.0	2.8
0.2	1.1	1.3	1.8	2.5	3.4
0.25	1.3	1.5	2.1	2.9	4.0
0.3	1.5	1.8	2.4	3.3	4.6
0.35	1.7	2.0	2.7	3.7	5.1
0.4	1.8	2.2	3.0	4.1	5.7
0.45	2.0	2.4	3.2	4.5	6.2
0.5	2.2	2.5	3.5	4.8	6.6
0.6	2.5	2.9	4.0	5.5	7.6
0.7	2.8	3.2	4.5	6.1	8.5
0.8	3.0	3.6	4.9	6.8	9.3
0.9	3.3	3.9	5.4	7.4	10.2
1.0	3.6	4.2	5.8	8.0	11.0
1.1	3.8	4.5	6.2	8.5	11.7
1.2	4.1	4.8	6.6	9.1	12.5
1.3	4.3	5.1	7.0	9.6	13.3
1.4	4.6	5.4	7.4	10.2	14.0
1.5	4.8	5.6	7.7	10.7	14.7
1.6	5.0	5.9	8.1	11.2	15.4
1.7	5.2	6.2	8.5	11.7	16.1
1.8	5.5	6.4	8.8	12.2	16.8
1.9	5.7	6.7	9.2	12.7	17.4
2.0	5.9	6.9	9.5	13.1	18.1
2.2	6.3	7.4	10.2	14.1	19.4
2.4	6.7	7.9	10.9	15.0	20.6
2.6	7.1	8.4	11.5	15.9	21.9
2.8	7.5	8.8	12.2	16.8	23.1
3.0	7.9	9.3	12.8	17.6	24.3

Flame height calculated from model developed by Cheney *et al.* (2012)

Spread distance for an accelerating point ignition fire

Table Sd

Spread distance (km)

Rate of fire spread (km/h)	Elapse time (min)					
	15	30	45	60	120	180
0.025	0.002	0.01	0.01	0.02	0.04	0.07
0.05	0.002	0.01	0.02	0.04	0.09	0.14
0.1	0.01	0.03	0.05	0.07	0.17	0.27
0.2	0.02	0.05	0.10	0.15	0.34	0.54
0.4	0.03	0.11	0.20	0.29	0.69	1.09
0.6	0.05	0.16	0.30	0.44	1.03	1.63
0.8	0.07	0.22	0.39	0.59	1.38	2.18
1.0	0.09	0.27	0.49	0.73	1.72	2.72
1.25	0.11	0.34	0.62	0.91	2.16	3.41
1.5	0.13	0.40	0.74	1.10	2.59	4.09
1.75	0.15	0.47	0.86	1.28	3.02	4.77
2.0	0.17	0.54	0.99	1.46	3.45	5.45
2.25	0.19	0.61	1.11	1.65	3.88	6.13
2.5	0.21	0.67	1.23	1.83	4.31	6.81
2.75	0.24	0.74	1.35	2.01	4.74	7.49
3.0	0.26	0.81	1.48	2.20	5.17	8.17
3.25	0.28	0.88	1.60	2.38	5.61	8.85
3.5	0.30	0.94	1.72	2.56	6.04	9.54
2.75	0.24	0.74	1.35	2.01	4.74	7.49
4.0	0.34	1.08	1.97	2.93	6.90	10.90
4.5	0.39	1.21	2.22	3.29	7.76	12.26
5.0	0.43	1.35	2.46	3.66	8.62	13.62
5.5	0.47	1.48	2.71	4.03	9.49	14.98
6.0	0.51	1.62	2.96	4.39	10.35	16.35
6.5	0.56	1.75	3.20	4.76	11.21	17.71
7.0	0.60	1.89	3.45	5.12	12.07	19.07
7.5	0.64	2.02	3.69	5.49	12.94	20.43

Table FInt

Interpretation of the six fireline intensities classes in the Fire Behaviour Characteristics Chart (inside front cover)

Based on AFDRS fire danger classes (after Matthews *et al.* 2019)

Fireline intensity (kW/m)	Fire behaviour and suppression interpretations
< 100	Marginal propagation. Fire difficult to ignite and sustain. Fires generally unlikely to spread and likely to self-extinguish at <10 kW/m.
100 – 750	Slow spreading f*ires*, typically involving surface and near-surface fuels and sometimes bark and elevated fuels. Spotting is sporadic and limited to short distances. Fires generally easy to suppress and contain.
750 – 4,000	Actively spreading fires typically involving surface, near-surface, elevated and bark fuel layers and occasionally canopy fuels through intermittent crowning. Low-moderate spotting frequency; isolated medium range spotting can occur. Fires typically suppressed with direct, parallel or indirect attack.
4,000 – 10,000	Rapidly spreading fires with potential for development into large burn areas within burning period. Fires typically involving all fuel layers. Short-range spotting is prevalent, with possibility of medium range and occasional long-range distance spotting. Increasing focus on defensive suppression strategies.
10,000 – 30,000	Fast moving fires involving the full fuel complex. Possibility of large fire area growth and strong convective plume development if conditions are maintained. Possibility for erratic strong winds and fire behaviour in localised areas. High density short- and medium-range spotting with possible isolated long-range spotting in the upper range of the class. Conditions limit strategic suppression options. High levels of threat to life and property. Elevated risk to firefighter safety and the community.
>30,000	Fast moving fires with flames taller than canopy. Profuse spotting dominating fire propagation, leading to increased spread of the fire. Fire storm, erratic conditions can develop. Long-range spotting distances greater than 10 km possible, creating new fast spreading fires. Strong convection column likely to form. Conditions limit strategic suppression options. High levels of threat to life and property. Spotting densities pose a severe risk to firefighter safety and the community.

11 Fire shape and flank propagation of wind driven fires

As a fire builds up from a point ignition and spreads across the landscape under the influence of wind speed, fuel moisture, fuel type and topography it typically adopts a roughly elliptical shape (Figure 32). The general shape of this ellipse, as defined by the ratio of its total length to maximum breadth, has been assumed in specific fuel types to be largely a function of the open wind speed. Stronger wind speeds will typically exert a greater dominance over fire propagation and shape, at times overwhelming the effect of other fire environmental variables. For a fire spreading over a heterogeneous landscape, this dependence on wind speed decreases with time since ignition as the fire spreads over different fuel types and topographies, is subject to changes in wind direction, and its main spread may be influenced by breaks in the fuel continuity or suppression actions that constrain propagation in sections of its perimeter.

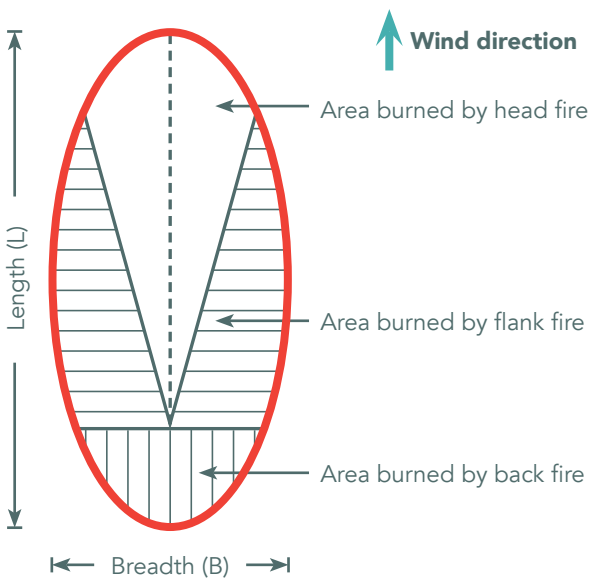

Figure 32. Schematic diagram of a simple elliptical fire growth model (after Van Wagner 1969). This ellipse has a length-to-breadth ratio (L:B) of 2:1

Table LB (inside back cover) gives the tabulated relationship between wind speed and the Length-to-Breadth ratio (L:B) for fires spreading from a point source in eucalypt forests under idealised conditions. Also included in this table are the associated flank fire spread factors based on the assumed L:B. These factors can be used to estimate the spread rate of flank fires. Simply multiply the forward rate of fire spread by the flank R factor to obtain the rate of spread for each flank of the fire.

Fire spread prediction worksheet example		
Fire name: The great fire of pontypandy	**Date:** 13 November 2021	
Fire spread period	*1*	
Prediction time interval:	*1400 to 1700*	← time duration of fire run
Fuel inputs		
Fuel type:	*Low prod., long unburned*	← from **Table F** or other source
Surface fuel load (t/ha)	*14*	← from **Table F** or other source
Understorey fuel height (m)	*0.5*	← from **Table F** or other source
Elevated fuel height (m)	*0.8*	← from **Table F** or other source
Weather inputs and moisture content		
Open wind speed (km/h)	*20*	← from weather forecast
Drought Factor	*8*	← from weather forecast
Air temperature (°C)	*34*	← from weather forecast
Relative humidity (%)	*20*	← from weather forecast
Fine dead moisture content (%)	*4.6*	← from **Table M1**
Fuel moisture effect	*0.93*	← from **Table Me**
Fire spread calculations		
Flat ground rate of fire spread (km/h)	*0.90 km/h*	← from **Table R3**
Slope steepness (° or %)	*0*	← from map or DEM
Overall rate of fire spread (km/h)	*0.90 km/h*	← 0.9 x 1 (from **Table S**)
Spread distance in period (km)	*2.7 km*	← 0.9 above x 3 h run duration
Map scale	*1:25,000*	← from map
Forward spread distance on map (cm)	*10.8 cm*	← distance in cm / map scale
Flank fire rate of spread (km/h)	*0.17 km/h*	← 0.9 x 0.19 (from **Table LB**)
Flank spread distance in period (km)	*0.51 km/h*	← 0.17 above x 3 h run duration
Flank spread distance on map (cm)	*2.0 cm*	← distance in cm / map scale
Observed rate of fire spread (km/h)		

Fire spread prediction worksheet		
Fire name:	Date:	
Prediction points	1	2
Prediction time interval:		
Fuel inputs		
Fuel type:		
Surface fuel load (t/ha)		
Understorey fuel height (m)		
Elevated fuel height (m)		
Weather inputs		
Open wind speed (km/h)		
Drought Factor		
Air temperature (°C)		
Relative humidity (%)		
Fine dead moisture content (%)		
Fuel moisture effect		
Fire spread calculations		
Flat ground rate of fire spread (km/h)		
Slope steepness (° or %)		
Overall rate of fire spread (km/h)		
Spread distance in period (km)		
Map scale		
Forward spread distance on map (cm)		
Flank fire rate of spread (km/h)		
Flank spread distance in period (km)		
Flank spread distance on map (cm)		
Observed rate of fire spread (km/h)		

References

Albini, F.A. (1976) Estimating Wildland Fire Behavior and Effects. US Department of Agriculture, Forest Service, Intermountain Forest and Range Experiment Station, General Technical Report INT-30, Ogden, Utah, USA. 92 pp.

Bureau of Meteorology (2014) Beaufort wind scale, Accessed 5 December 2014, http://www.bom.gov.au/lam/glossary/beaufort.shtml

Cawson JG, Hemming V, Ackland A, Anderson W, Bowman D, Bradstock R, Brown TP, Burton J, Cary GJ, Duff TJ, Filkov A, Furlaud JM, Gazzard T, Kilinc M, Nyman P, Peacock R, Ryan M, Sharples J, Sheridan G, Tolhurst K, Wells T, Zylstra P, Penman TD (2020) Exploring the key drivers of forest flammability in wet eucalypt forests using expert-derived conceptual models. *Landscape Ecology* 35, 1775-1798.

Cheney NP, Bary GAV (1969) The propagation of mass conflagrations in a standing eucalypt forest by the spotting process. In: Collected Papers (Paper A6), Mass Fire Symposium, Volume I. Commonwealth of Australia, Defence Standards Laboratory, Maribyrnong, Vic, Australia. 18 pp.

Cheney NP, Gould JS, McCaw WL, Anderson WR (2012). Predicting fire behaviour in dry eucalypt forest in southern Australia. *Forest Ecology and Management* 280, 120-131.

Cruz MG, Alexander ME (2013) Uncertainty associated with model predictions of surface and crown fire rates of spread. *Environmental Modelling & Software* 47, 16-28.

Cruz MG, Alexander ME, Fernandes PM, Kilinc M, Sil Â (2020) Evaluating the 10% wind speed rule of thumb for estimating a wildfire's forward rate of spread against an extensive independent set of observations. *Environmental Modelling & Software* 133, 104818. 15 pp.

Cruz MG, Cheney NP, Gould JS, McCaw WL, Kilinc M, Sullivan AL (2022) An empirical-based model for predicting the forward spread rate of wildfires in eucalypt forests. *International Journal of Wildland Fire. In press.*

Cruz MG, Gould JS, Alexander ME, Sullivan AL, McCaw WL, Matthews S, 2015. *A Guide to Rate of Fire Spread Models for Australian Vegetation*. Revised edition. CSIRO and AFAC, Melbourne, Vic, Australia. 125 pp.

Cruz MG, Sullivan AL, Gould JS, Sims NC, Bannister AJ, Hollis JJ and Hurley RJ (2012) Anatomy of a catastrophic wildfire: The Black Saturday Kilmore East fire in Victoria, Australia. *Forest Ecology and Management* 284, 269-285.

Duff TJ, Cawson JG, Cirulis B, Nyman P, Sheridan GJ, Tolhurst KG (2018) Conditional Performance Evaluation: Using Wildfire Observations for Systematic Fire Simulator Development. *Forests* 9, 189.

Gould JS, McCaw WL, Cheney NP, Ellis PF, Knight IK, Sullivan AL (2007a) Project Vesta: fire in dry eucalypt forest : fuel structure, fuel dynamics and fire behaviour. Ensis-CSIRO, Canberra, ACT and Department of Environment and Conservation, Perth, WA, Australia. 218 pp.

Gould JS, McCaw WL, Cheney NP, Ellis PF, Matthews S (2007b) Field Guide: Fuel assessment and fire behaviour prediction in dry eucalypt forest. (Ensis-CSIRO, Canberra ACT, and Department of Environment and Conservation, Perth, WA, Australia. 92 pp.

Hodgson A (1967) Control burning in eucalypt forests in Victoria, Australia. Journal of Forestry 66, 601-605.

Keetch JJ, Byram GM (1968) A drought index for forest fire control. U.S. Department of Agriculture, Forest Service, Southeast Forest Experiment Station, Research Paper SE-38, Asheville, North Carolina, U.S.A. 32 pp. (revised November 1988.)

Luke RH, McArthur AG (1978) *Bushfires in Australia*. Australian Government Publishing Service, Canberra, ACT, Australia. 359 pp.

Matthews S (2006) A process-based model of fine fuel moisture. *International Journal of Wildland* Fire 15, 155-168.

Matthews S, Fox-Hughes P, Grootemaat S, Hollis JJ, Kenny BJ, Sauvage S (2019) Australian Fire Danger Rating System: Research Prototype, NSW Rural Fire Service, Lidcombe, NSW, Australia. 384 pp.

McArthur AG (1962) Control Burning in Eucalypt Forests. Forestry and Timber Bureau Leaflet 80, Forest Research Institute, Canberra, ACT, Australia. 31 pp.

McArthur AG (1966) The application of a drought index system to Australia fire control. Forestry and Timber Bureau, Forest Research Institute, Canberra, ACT, Australia. 18 pp.

McArthur AG (1967) Fire Behaviour in Eucalypt Forests. Forestry and Timber Bureau Leaflet 107. Forest Research Institute, Canberra, ACT, Australia. 36 pp.

McArthur AG (1969) The fire control problem and fire research in Australia. In: Proceedings of the 1966 Sixth World Forestry Congress, vol. 2. Spanish Minister of Agriculture, Madrid, Spain. pp. 1986–1991.

McArthur AG, Luke RH (1963) Fire behaviour studies in Australia. *Fire Control Notes* 24(4), 87-92.

Moon K, Duff TJ, Tolhurst KG (2019) Sub-canopy forest winds: understanding wind profiles for fire behaviour simulation. *Fire Safety Journal* 105, 320-329.

Pickering BJ, Duff TJ, Baillie C, Cawson JG (2021) Darker, cooler, wetter: forest understories influence surface fuel moisture. *Agricultural and Forest Meteorology* 300, 108311.

Rawson RP, Billing PR, Duncan SF (1983) The 1982-83 forest fires in Victoria. *Australian Forestry* 46, 163-172.

Rothermel RC (1983) How to Predict the Spread and Intensity of Forest and Range fires. US Department of Agriculture, Forest Service, Intermountain Forest and Range Experiment Station, General Technical Report INT-143, Ogden, Utah, USA. 161 pp.

Slijepcevic A, Anderson WR, Matthews S, Anderson DH (2018) An analysis of the effect of aspect and vegetation type on fine fuel moisture content in eucalypt forest. *International Journal of Wildland Fire* 27, 190-202.

Sneeuwjagt RJ, Peet GB (1985) Forest Fire Behaviour Tables for Western Australia, third ed. Department of Conservation and Land Management, Perth, WA, Australia. 59 pp.

Storey MA, Price OF, Bradstock RA, Sharples JJ (2020) Analysis of variation in distance, number, and distribution of spotting in southeast Australian wildfires. *Fire* 3, 10.

Sullivan AL, Sharples JJ, Matthews S, Plucinski MP (2014) A downslope fire spread correction factor based on landscape-scale fire behaviour. *Environmental Modelling & Software* 62, 153-163.

Taylor SW, Alexander ME (2018) A field guide to the Canadian Forest Fire Behavior Prediction (FBP) System. 3rd edition. Natural Resources Canada, Canadian Forest Service, Northern Forestry Centre, Edmonton, Alberta, Canada. Special Report 11. 101 pp.

Tolhurst KG, Shields B, Chong D (2008) Phoenix: development and application of a bushfire risk management tool. *Australian Journal of Emergency Management* 23, 47-54.

Van Wagner, CE (1969) A simple fire growth model. *The Forestry Chronicle* 45, 103-104.

Walker J (1981) Fuel dynamics in Australian vegetation. In: AM Gill, RH Groves, IR Noble (Eds), *Fire and the Australian Biota*. Australian Academy of Science, Canberra. pp. 101-128.

Amicus

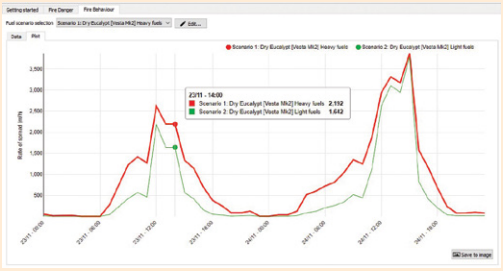

Amicus is a software-based fire behaviour prediction system developed by CSIRO. It is designed to enable fast and reliable bushfire spread predictions, calculating key fire behaviour characteristics (*e.g.*, rate of spread, flame height, fireline intensity, maximum spotting distance). It implements up to date fires behaviour models for Australia's major vegetation types (*e.g.*, grasslands, shrublands, dry and wet eucalypt forests, and industrial plantations).

Users provide information about the location of the prediction, including the topography, the weather and fuel characteristics. Amicus generates predictions in tabular and graphical formats with warnings when the inputs for the selected model are outside of the model's guidelines. These warnings act as alerts for increased uncertainty in any predictions made during these conditions. The current version of Amicus incorporates the Vesta Mk 2 model for dry and wet eucalypt forests.

Amicus is freely-available. It can be downloaded from https://research.csiro.au/amicus/

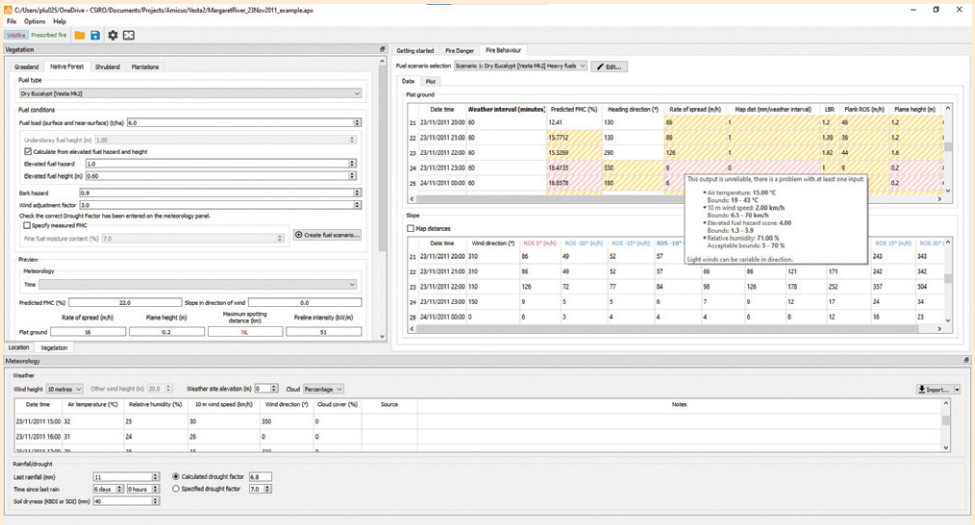

Modified Beaufort wind scale

Beaufort scale number	Descriptive term	10-m open wind speed (km/h)	Description on land
0	Calm	<1	Smoke rises vertically.
1	Light air	1 – 5	Smoke drift indicates wind direction. Leaves and wind vanes are stationary.
2	Light wind	6 – 11	Wind felt on exposed skin. Leaves rustle. Wind vanes begin to move.
3	Gentle wind	12 - 19	Leaves and small twigs constantly moving, light flags extended.
4	Moderate winds	20 - 29	Raises dust and loose paper; small branches are moved.
5	Fresh winds	30 - 39	Small trees in leaf begin to sway; crested wavelets form on inland waters
6	Strong winds	40 - 50	Large branches in motion; whistling heard in telephone wires.
7	Near gale	51 - 62	Whole trees in motion; inconvenience felt when walking against wind.
8	Gale	63 - 75	Twigs break off trees; progress generally impeded.
9	Strong gale	76 - 87	Slight structural damage occurs – roofing dislodged; larger branches break off.
10	Storm	88 - 102	Seldom experienced inland; trees uprooted; considerable structural damage.

(adapted from Bureau of Meteorology, 2014)

Table LB. Length-to-breadth (LB) ratio for elliptical fire shapes on level terrain

10-m open wind speed (km/h)										
0	5	10	15	20	25	30	35	40	45	50
L:B										
1.0	1.1	1.5	2.0	2.6	3.3	3.8	4.4	5.0	5.6	6.1
Flank R factor (fraction of forward R)										
1.0	0.45	0.33	0.25	0.19	0.15	0.13	0.11	0.10	0.09	0.08

Applicable to level terrain (adapted from Taylor and Alexander 2018)

Scale distances (km)

0 cm	1:10,000	1:25,000	1:50,000
	0.1	0.25	0.5
	0.2	0.50	1.0
	0.3	0.75	1.5
	0.4	1.0	2.0
5 cm	0.5	1.25	2.5
	0.6	1.5	3.0
	0.7	1.75	3.5
	0.8	2.0	4.0
	0.9	2.25	4.5
10 cm	1.0	2.5	5.0
	1.1	2.75	5.5
	1.2	3.0	6.0
	1.3	3.25	6.5
	1.4	3.5	7.0
15 cm	1.5	3.75	7.5

"Can wildland fire behaviour really be predicted? That depends on how accurate you expect the prediction to be. The minute-by-minute movement of a fire will probably never be predictable—certainly not from weather conditions forecasted many hours before the fire. Nevertheless, practice and experienced judgment in assessing the fire environment, coupled with a systematic method of calculating fire behaviour, yield surprisingly good results."

R. C. Rothermel (1983)